

**MEASUREMENT OF THE AVERAGE RADIATION DOSE TO PATIENTS DURING  
INTRACRANIAL ANEURYSM COIL EMBOLIZATION**

**By**

**YANDA PETER**

**Thesis submitted in fulfilment of the requirements for the degree**

**Master of Science: Radiography**

**In the Department of Medical Imaging and Therapeutic Sciences**

**Faculty of Health and Wellness Sciences, Bellville Campus,**

**Cape Peninsula University of Technology**

**Supervisor: Mr A. Speelman**

**Co-supervisors: Mrs V. Daries**

**Mr V. Jonas**

28 August 2019

**CPUT copyright information**

This dissertation/thesis may not be published either in part (in scholarly, scientific or technical journals), or as a whole (as a monograph), unless permission has been obtained from the University.

## **DECLARATION**

I, Yanda Peter, declare that the contents of this dissertation/thesis represent my own unaided work, and that the dissertation/thesis has not previously been submitted for academic examination towards any qualification. Furthermore, it represents my own opinions and not necessarily those of the Cape Peninsula University of Technology.



28 August 2019

---

**Signed**

---

**Date**

## **ACKNOWLEDGEMENTS**

### **I wish to thank:**

- First and foremost, God my creator, for giving me strength and wisdom during challenging times.
- My family for their continued support and love.
- My research supervisors, Mr Aladdin Speelman, Mrs Valdiela Daries and Mr Vuyisile Jonas, for their support and guidance.
- Dr Tobie Kotze for his valuable contribution.
- My mentor, Mrs Carol Le Roux, for always being supportive.
- Ms Cherral Bourne for agreeing to be my research assistant and her contribution during the data collection.
- Mr Dewald Basson for translating the consent form from English to Afrikaans.
- The Medical Physics Department at the research site for allowing me to use their resources for this research study.
- The Vascular and Interventional Radiology Department radiographers and neuro-interventionalists at the research site for always being willing to help.
- Lastly, I would like to acknowledge the University Research Fund for financial assistance.

## ABSTRACT

**Introduction:** Intracranial aneurysm coil embolization is a fluoroscopically guided interventional procedure that is often preferred over surgical clipping for the treatment of intracranial aneurysms. Fluoroscopically guided procedures are associated with high levels of radiation doses which have the potential to induce skin injuries; and this necessitates adherence to radiation protection measures, especially the optimization of radiation exposure during fluoroscopically guided procedures. Optimization of radiation exposure can be achieved by applying the “as low as reasonably achievable” (ALARA) principle and by implementing diagnostic reference levels (DRLs). Monitoring and documentation of radiation doses at the end of each procedure is also essential to identify patients that are at risk of developing radiation-induced injuries for possible follow-up.

**Aim:** This research study aimed to determine the average radiation dose to patients’ thyroid glands and skin during intracranial aneurysm coil embolization. The objectives were to establish preliminary DRLs for intracranial aneurysm coil embolization; to ascertain whether the anatomical location of the intracranial aneurysm had an effect on the radiation dose and to compare the measured thyroid gland and skin doses to the Monte Carlo calculated doses.

**Methods:** A prospective quantitative research study was conducted on 34 participants who had intracranial aneurysms that required coil embolization during the study period. Radiation doses to the anterior neck of participants, over the thyroid gland region, were measured using lithium fluoride thermoluminescent dosimeters (TLDs). In addition, the air-kerma area product (KAP) values were used to determine the participants’ skin dose and the DRLs. Considering that it is not possible to perform direct thyroid measurements on human beings, phantom-based simulation studies were performed to evaluate the difference between the dose measured on the anterior neck and the dose measured directly on the thyroid gland. Three different aneurysm coil embolization scenarios were simulated during the phantom-based simulation studies. TLDs were placed on the anterior neck and in the thyroid hole of the phantom, which represents the anatomical location of the thyroid gland, during each simulation. The thyroid and skin doses were also calculated using a Monte Carlo program. The measured thyroid gland and skin doses were compared to the doses obtained from Monte Carlo calculations.

**Results:** The average percentage difference between the anterior neck doses and thyroid radiation doses was found to be 61%. This value was added to the radiation dose measured on the anterior neck of participants to obtain the thyroid absorbed doses during coil embolization procedures. The thyroid absorbed doses ranged between 3.2 and 20.95 mGy with a mean of 11.25 mGy. The KAP values ranged between 33 and 125 Gy.cm<sup>2</sup>. The DRL established during this study was 68 Gy.cm<sup>2</sup>, 616 image frames and 30 minutes of fluoroscopy time. There was no agreement between measured thyroid dose and calculated thyroid doses while there was strong positive correlation between measured and calculated skin doses. The results showed no statistically significant relationship between aneurysm location and the radiation dose.

**Conclusion:** The skin doses in this research study were below the threshold doses suggested in the literature for deterministic effects of radiation. The study results therefore suggest that patients that undergo intracranial aneurysm coil embolization at the research site are not at risk of developing radiation-induced skin injuries. The established DRLs were also lower than internationally published DRLs for intracranial aneurysm coil embolization.

**Keywords:** Intracranial aneurysm coil embolization, Radiation dose, Diagnostic Reference level, Thermoluminescent dosimeter, Air-kerma area product

## LIST OF ABBREVIATIONS

AEC	Automatic Exposure Control
Al	Aluminium
ALARA	As Low As Reasonably Achievable
BRAT	Barrow Ruptured Aneurysm Trial
CARE	Combined Applications to Reduce Exposure
CLARITY	Clinical and Anatomical Results in the Treatment of Ruptured Intracranial Aneurysms
CT	Computed Tomography
CTA	Computed Tomography Angiography
CTB	Computed Tomography of the Brain
DAP	Dose Area Product
DNA	Deoxyribonucleic acid
DRL	Diagnostic Reference Level
DSA	Digital Subtraction Angiography
ECC	Element Correction Coefficient
FDA	Food and Drug Administration
FSD	Focal spot to Skin Distance
Gy	Gray
Gy.cm <sup>2</sup>	Gray-centimetres squared
HPCSA	Health Professions Council of South Africa
HVL	Half Value Layer
IAEA	International Atomic Energy Agency
ICRP	International Commission on Radiological Protection

ICRU	International Commission on Radiation Units and Measurements
ISAT	International Subarachnoid Aneurysm Trial
KAP	Air-kerma Area Product
KERMA	Kinetic Energy Released in Matter
kV	Kilovoltage
LiF:Mg,Ti	Lithium fluoride doped in magnesium and titanium
mAs	Milli-ampere per second
mGy	Milli-gray
$\mu$ Gy	Micro-gray
MSD	Maximum Skin Dose
NCRP	National Council on Radiation Protection and Measurements
PACS	Picture Archiving and Communication System
PBSS	Phantom-Based Simulated Studies
PCXMC	Personal Computer program for X-ray Monte Carlo
RSSA	Radiological Society of South Africa
SAH	Subarachnoid Haemorrhage
SORSA	Society of Radiographers of South Africa
Sv	Sievert
TLD	Thermoluminescent Dosimeter
WHO	World Health Organization
WMA	World Medical Association
$W_R$	Radiation weighting factor
$W_T$	Tissue weighting factor

## Table of Contents

<b>DECLARATION</b>	<b>i</b>
<b>ACKNOWLEDGEMENTS</b>	<b>ii</b>
<b>ABSTRACT</b>	<b>iii</b>
<b>LIST OF ABBREVIATIONS</b>	<b>v</b>
<b>CHAPTER 1: INTRODUCTION</b>	<b>1</b>
1.1. Background	1
1.2. Problem statement	3
1.3. Research question and objectives	3
1.4. Significance of the study	4
1.5. Overview of the methodology	5
1.6. Conclusion	6
<b>CHAPTER 2: LITERATURE REVIEW</b>	<b>7</b>
2.1. Introduction	7
2.2. Interventional procedures	7
2.2.1. Intracranial aneurysms .....	8
2.3. Biological effects of radiation	9
2.3.1. Stochastic effects .....	10
2.3.2. Radiation effects to the thyroid gland.....	10
2.3.3. Deterministic effects .....	11
2.3.4. Radiation effects on the skin.....	11
2.4. Radiation dosimetry	13
2.4.1. Absorbed dose .....	14
2.4.2. Equivalent dose.....	14
2.4.3. Thermoluminescent dosimeters.....	15
2.4.3.1. TLD calibration .....	16
2.4.3.2. TLD read out and annealing .....	17
2.4.4. Air-kerma area product meter.....	18
2.4.5. Skin dose assessment.....	18
2.4.6. Monte Carlo calculations .....	20
2.5. Justification and optimization of dose	21
2.6. Diagnostic reference levels	22
2.6.1. Published DRLs for intracranial aneurysm coiling procedures .....	24
2.6.2. DRLs in South Africa .....	25
2.6.2.1 DRLs for fluoroscopy procedures in South Africa.....	26
2.6.2.2. DRLs for angiography and interventional procedures in South Africa .....	26



2.7. Effect of the aneurysm location on radiation dose	27
2.8. Conclusion	28
<b>CHAPTER 3: RESEARCH METHODOLOGY</b>	29
3.1. Research question and objectives	29
3.2. Research methods	29
3.3. Research study site	29
3.4. Research population	30
3.4.1. Inclusion criteria .....	30
3.4.2. Exclusion criteria .....	30
3.4.3. Sampling .....	30
3.4.4. Sample size.....	31
3.5. Dose measurement materials	31
3.5.1. Thermoluminescent dosimeters.....	31
3.5.1.1. TLD calibration materials .....	31
3.5.1.2. TLD calibration procedure .....	32
3.6. Dose measurement methods	34
3.6.1. Actual coil embolization study.....	34
3.6.2. Phantom-based simulation studies .....	36
3.7. Equipment	38
3.7.1. Intracranial aneurysm embolization equipment.....	38
3.7.2. TLD reader .....	39
3.7.3. TLD annealing oven .....	40
3.8. Dose calculations	41
3.8.1. Thyroid absorbed dose.....	41
3.8.2. Thyroid equivalent dose .....	41
3.8.3. Diagnostic Reference Levels .....	41
3.8.4. Monte Carlo calculations .....	42
3.9. Data collection and analysis	43
3.10. Ethical considerations	43
3.11. Conclusion	45
<b>CHAPTER 4: RESULTS</b>	46
4.1. Introduction	46
4.2. Data analysis	47
4.2.1. Descriptive statistics .....	47
4.2.2. Inferential statistics.....	48
4.3. Phantom-based simulation studies (PBSS)	49
4.4. Radiation dose to the thyroid gland	52
4.4.1 Thyroid absorbed doses .....	52
4.4.2. Thyroid equivalent doses.....	54

4.4.3. Monte Carlo calculated thyroid doses.....	54
4.5. Radiation dose to the skin	55
4.5.1. Radiation dose to the skin as determined by the KAP meter .....	55
4.5.2. Monte Carlo calculated skin doses .....	57
4.6. Effect of aneurysm location on the radiation dose	58
4.7. Diagnostic reference levels	61
4.8. Correlation between KAP and the number of image frames	62
4.9. Correlation between KAP and the maximum entrance skin dose	62
4.10. Conclusion	64
<b>CHAPTER 5: DISCUSSION</b>	<b>65</b>
5.1. Introduction	65
5.2. Sensitivity of TLDs	65
5.3. Validity and reliability of data	66
5.4. Thyroid radiation doses	67
5.5. Skin radiation doses	68
5.6. Effect of aneurysm location on radiation dose	69
5.7. Diagnostic reference levels	70
5.8. Comparison between measured and calculated doses	72
5.9. Conclusion	73
5.10. Limitations and recommendations	75
<b>REFERENCES</b>	<b>77</b>
<b>LIST OF FIGURES</b>	
Figure 2.1: Digital subtraction cerebral angiography image showing an aneurysm	9
Figure 3.1: A PTW-Freiburg ionization chamber	32
Figure 3.2: Ionization chamber connected to a PTW UNIDOS electrometer for TLD calibration	33
Figure 3.3: Encapsulated TLDs on a polyethylene foam pad for calibration	33
Figure 3.4: Simulated TLD positioning on patients	35
Figure 3.5: RANDO phantom images	36
Figure 3.6: TLD positioning on the phantom	38
Figure 3.7: Siemens Artiz Zee biplane angiography unit	39
Figure 3.8: REXON TLD reader	40
Figure 3.9: A PTW-Freiburg TLD annealing oven	41
Figure 4.1: Age distribution of research participants	48
Figure 4.2: Results of the phantom-based simulation studies	51
Figure 4.3: Comparison between TLD measured and PCXMC calculated thyroid doses	55
Figure 4.4: Power fit between measured and calculated skin dose	57
Figure 4.5: Linear fit between measured and calculated skin dose	58

Figure 4.6: Pie chart showing aneurysm location distribution	59
Figure 4.7: Scatter graph showing relationship between KAP and number of image frames	62
Figure 4.8: Scatter graph showing correlation between KAP and maximum entrance skin dose	64

## LIST OF TABLES

Table 2.1: Radiation effects on the skin	12
Table 2.2: KAP threshold values for radiation effects on the skin	12
Table 2.3: Radiation weighting factors	14
Table 2.4: Tissue weighting factors	15
Table 2.5: A summary of published DRLs for intracranial aneurysm coiling	24
Table 3.1: Imaging data for simulated phantom studies	37
Table 3.2: Parameters used for dose calculation in the PCXMC program	42
Table 4.1: Measurements obtained from phantom-based simulation studies	50
Table 4.2: Anterior neck doses from TLD measurements and calculated thyroid absorbed doses to participants	53
Table 4.3: Thyroid absorbed doses to participants	54
Table 4.4: KAP values from the current study	56
Table 4.5: KAP values according to type of procedure	56
Table 4.6: The thyroid absorbed doses and KAP values for different aneurysm locations	60
Table 4.7: DRLs for intracranial aneurysm coil embolization	61
Table 4.8: KAP and maximum entrance skin dose values	63
Table 5.1: Thyroid doses in cerebral embolizations obtained from current study and published studies	67
Table 5.2: KAP values from the current study and published studies	69
Table 5.3: Comparison of the DRL from the current study with DRLs for intracranial aneurysm coiling from published international studies	71
Table 5.4: Comparison of the DRL from the current study with DRLs for cerebral embolization from South Africa	72

## APPENDICES

Appendix A: Ionization chamber and electrometer calibration certificates
Appendix B1: Actual coil embolization study data collection sheet
Appendix B2: Phantom-based simulation study data collection sheet
Appendix C1: CPUT ethics certificate
Appendix C2: UCT ethics certificate
Appendix C3: Research site permission letter
Appendix D: Informed consent form

## **CHAPTER 1: INTRODUCTION**

### **1.1. Background**

Intracranial aneurysms occur as a result of weakened blood vessel walls due to atherosclerosis, trauma, infection, congenital defects or high blood pressure (Kowalczyk, 2014:126; Linn-Watson, 2014:219). Patients with ruptured intracranial aneurysms present with subarachnoid haemorrhage (SAH) which accounts for about 75% of all SAH. The most common type of intracranial aneurysm is the degenerative saccular aneurysm (Kowalczyk, 2014:126; Rodriguez-Regent et al., 2014); and the common locations are the anterior communicating artery, origin of posterior communicating artery, middle cerebral artery and basilar artery (Rodriguez-Regent et al., 2014). According to Sandborg et al. (2012), intracranial aneurysms are more common in females than in males and occur between the ages of 40 and 60 years, with a mortality rate of 45%.

SAH is often diagnosed on uncontrasted Computed Tomography of the brain (CTB). Following the confirmation of SAH on CTB, a cerebral Computed Tomography Angiography (CTA) is done to detect the presence of intracranial aneurysms (Sandborg et al., 2012). Digital subtraction angiography (DSA) can also be employed to diagnose intracranial aneurysms. Due to its invasiveness, DSA is usually reserved for aneurysms smaller than 3 mm that are sometimes missed on cerebral CTA, as well as therapeutic angiographic procedures (Rodriguez-Regent et al., 2014).

There are two treatment options for intracranial aneurysms: endovascular coil embolization and surgical clipping of the aneurysm. Following the results of the International Subarachnoid Aneurysm Trial (ISAT) that indicated that endovascular coil embolization has better patient outcomes than surgical clipping, there has been an increase in the number of endovascular embolization cases worldwide (Zhao et al., 2018). Endovascular coil embolization is a fluoroscopically guided interventional procedure associated with high levels of radiation. The increase in the number of endovascular cases raises concern about the amount of radiation to the patients and the associated radiation risks (Shortt et al., 2007).

The harmful effect of x-rays on the human body is due to the ionization of atoms caused by the deposition of radiation energy on the tissues within the radiation beam. The radiation effects to

the irradiated individual are termed somatic effects and are divided into stochastic and deterministic effects (Hall, 2012:3).

Stochastic effects are radiation effects which do not have a minimum dose below which they do not occur, or a maximum dose above which they are sure to occur. Stochastic effects occur by chance; and the chances of their occurrence increase with the increase in radiation dose. Deterministic effects, on the other hand, have a threshold dose above which they occur, and the severity of the effect increases with an increase in the radiation dose. Although rare, deterministic effects can occur following complex interventional procedures (National Council on Radiation Protection and Measurements, NCRP, 2011). The organs most likely to be affected by radiation during intracranial aneurysm coil embolization are the eyes and the thyroid gland. This is due to these organs' radiosensitivity and their proximity to the radiation beam during intracranial aneurysm coil embolization. The skin on the face and neck, as well as the scalp, is also exposed to radiation during intracranial aneurysm coil embolization (Shortt et al., 2007; Miller et al., 2010).

To minimize the harmful effects of radiation, it is vital to apply radiation protection measures, especially for procedures like fluoroscopically guided interventions. The two principles of radiation protection in medical exposure are justification and optimization of exposure. The principle of justification means that the radiation exposure should only be carried out when there is sufficient benefit to the patient while optimization entails ensuring that, for justified procedures, the radiation exposure is optimised so as to maximise the benefit to the patients while keeping the radiation risks low (International Commission on Radiological Protection, ICRP, 2007). One of the methods of applying the optimization principle is the use of diagnostic reference levels (DRLs). DRLs were introduced by the ICRP in 1996 as a dose management tool against which patient doses are compared to identify abnormal levels of radiation. According to the ICRP recommendations, DRLs should be set for common examinations with low and high radiation doses, as well as all procedures with high radiation doses (ICRP, 2017).

This research study established preliminary DRLs for intracranial aneurysm coil embolization and determined the radiation doses to the thyroid glands and skin of patients undergoing endovascular coil embolization of intracranial aneurysms at an academic hospital in Cape Town, South Africa.

## **1.2. Problem statement**

Interventional procedures are among radiological examinations that contribute the highest radiation doses in medical radiation. In the United States, interventional procedures are the third highest contributors to medical radiation dose after CT and nuclear medicine procedures (Hall, 2012:247). Although endovascular aneurysm coil embolization has clinical benefits to patients with aneurysmal SAH, this procedure comes with a disadvantage of increased radiation dose to the patients, especially over the head area (Sandborg et al., 2012).

The thyroid gland is one of the radiosensitive organs usually positioned within or close to the radiation field during intracranial aneurysm coil embolization. Radiation to this organ is associated with thyroid cancer (Shortt et al. 2007). The eyes are also exposed to radiation during intracranial aneurysm coil embolization, however radiation effects and measurement of the radiation dose to the eyes were not part of the current research. The skin on the face and the scalp is also exposed to radiation during intracranial aneurysm coil embolization. Prolonged radiation to the skin can result in skin injuries. Although the scalp does not suffer skin damage, the hair of the scalp is more sensitive to epilation than hair on other parts of the body (Miller et al., 2010). Previous studies conducted by Theodorakou and Horrocks (2003), Suzuki et al. (2008) and Sandborg et al. (2012) found that the threshold dose for erythema and epilation can be exceeded during neuro-embolization procedures and epilation was reported in some patients. The possibility of exceeding threshold doses for deterministic effects raised concern about the amount of radiation patients are exposed to during intracranial aneurysm coil embolization at the research site. There were also no DRLs for intracranial aneurysm embolization procedures at the research site, despite the ICRP's recommendations and the International Atomic Energy Agency (IAEA) and World Health Organization's (WHO) Bonn Call for Action.

## **1.3. Research question and objectives**

The research question for this study was: "What is the average radiation dose to patients undergoing intracranial aneurysm coil embolization?" This study aimed to determine the radiation dose to the patients' thyroid glands and skin during intracranial aneurysm coil embolization at an academic hospital in Cape Town, South Africa.

The research objectives of the study were to:

- Determine the radiation dose to patients' thyroid glands using TLDs and skin by means of a KAP meter during intracranial aneurysm coil embolization.
- Ascertain whether the anatomical location of the intracranial aneurysm affects the radiation dose to the patients.
- Establish preliminary diagnostic reference levels for intracranial aneurysm coil embolization.
- Compare measured thyroid gland and skin doses to thyroid gland and skin doses using the PCXMC program.

#### **1.4. Significance of the study**

Intracranial aneurysm coil embolization is associated with high levels of radiation, especially to the radiosensitive organs that are usually in or close to the radiation beam during these procedures. These radiosensitive organs include the skin, the thyroid gland and the eyes (Shortt et al., 2007). The high levels of radiation necessitate proper radiation dose management during intracranial aneurysm coiling to reduce the risk of possible radiation effects to the aforementioned tissues or organs. As part of radiation dose management, it is necessary to understand the levels of radiation dose received from radiological procedures so that radiation dose reduction measures can be employed when necessary (Miller et al., 2010). For this research study, it was therefore important to determine the radiation dose received by patients undergoing intracranial aneurysm coil embolization, as no previous studies have been performed to measure radiation dose during these procedures at the research site. Nationally, as far as could be established, there have also been no published studies on radiation doses received from intracranial aneurysm coil embolization procedures. The data obtained could be used to assess whether the dose patients receive during this interventional procedure at the research site is comparable to that reported in previous studies performed internationally. The results could also be used to optimise the intracranial aneurysm coil embolization procedures to ensure adherence to the ALARA principle.

As part of the Bonn Call for Action, WHO and IAEA called for the development and use of DRLs to promote the optimization of radiation exposure during radiological and interventional procedures (WHO, 2014). The DRLs provide data on the average radiation doses received during different procedures and can be used as quality assurance measures to identify equipment and protocols that produce high levels of radiation for correction. Thus, DRLs are guidance levels and not dose limits (ICRP, 2017). There are currently no diagnostic reference

levels for intracranial aneurysm coil embolization procedures at the research site. Also, according to what the researcher could find, there is only one peer reviewed published study on DRLs for cerebral interventions in South Africa. That is a study by Makosa and Conradie (2015). One of the objectives of the current study was to establish DRLs for intracranial aneurysm coil embolization procedures. The third quartile of air-kerma area product (KAP) values, number of image frames and fluoroscopy time obtained from this study are recommended for use as the DRLs at the research site.

Another objective of this study was to ascertain whether the anatomical location of the intracranial aneurysm affects the radiation dose to the patients. While there are many published studies internationally on radiation doses during intracranial aneurysm coil embolization, no previous studies that focused on the effect of aneurysm location on the radiation dose could be found. This suggests, therefore, that the current study is the first one to look at the relationship between the aneurysm location and radiation dose.

### **1.5. Overview of the methodology**

The study design consisted of three components. The first component was a quantitative, prospective study where the radiation dose to participants undergoing intracranial aneurysm coil embolization in the vascular and interventional laboratory within the radiography department at the research site was measured. The second component entailed measurement of the radiation dose during simulation of intracranial aneurysm coil embolization procedures on a human tissue equivalent phantom. The third component involved calculation of thyroid gland and skin doses received by patients during intracranial aneurysm coil embolization procedures using a Monte Carlo method.

Radiation dose to participants that had intracranial aneurysm coil embolization procedures was measured using thermoluminescent dosimeters (TLDs) positioned on the participants' anterior neck over the thyroid gland region. KAP was also used to determine the radiation dose to the participants' skin. DRLs for intracranial aneurysm embolization procedures were also established using the third quartile of the KAP values, the fluoroscopy time and the number of image frames. The aneurysm location, KAP value, fluoroscopy time, exposure factors, TLD readings, number of exposures and number of image frames, as well as the participants' gender and age, were recorded during this study.



During the phantom-based simulation studies (PBSS), the radiation dose was measured using TLDs positioned on the anterior neck of the phantom, as well as in the thyroid hole (which represents the anatomical location of the thyroid gland) of the phantom. The purpose of the PBSS was to determine the difference between the radiation dose measured on the anterior neck over the thyroid gland region and the dose measured at the anatomical location of the thyroid gland, as it is not possible to perform direct thyroid measurements on humans. KAP, fluoroscopy time, anterior neck TLD readings and thyroid TLD readings were recorded during the PBSS. The data were analysed to establish the difference between the anterior neck TLD reading and the thyroid TLD reading that was used to calculate the thyroid absorbed dose of participants.

The thyroid gland and skin doses were also calculated using the Monte Carlo method. The KAP, kilovoltage (kV), x-ray field size, focal spot to skin distance (FSD) and x-ray beam angulations documented during the actual coil embolization study were used for the Monte Carlo calculations. The results obtained from these calculations were compared to the dose values obtained from the TLD and KAP measurements to determine whether there was correlation between the measured and calculated doses.

Throughout this thesis, the radiation dose measured on the anterior neck over the thyroid gland region will be referred to as 'the anterior neck dose', while the dose measured at the anatomical location of the thyroid gland will be referred to as 'the thyroid dose'.

## **1.6. Conclusion**

This chapter has given an overview of the study background, the problem statement, the aims and objectives of the study as well as the significance of the study. The next chapter discusses the literature related to the aims and objectives of the study. Some of the topics that will be discussed in the literature review include radiation doses from interventional procedures, radiation dosimetry, effects of radiation on the skin and thyroid gland, as well as DRLs.

## **CHAPTER 2: LITERATURE REVIEW**

### **2.1. Introduction**

Interventional procedures are fluoroscopically guided procedures which are associated with high levels of radiation exposure. It is thus crucial to optimize radiation exposure during these procedures to minimize the deterministic effects on the patients (IAEA, 2010). Radiation dose optimization includes selection of appropriate equipment (for example, equipment with dose reduction technology) and appropriate use thereof which includes training of operators on the safe and appropriate use, as well as regular quality assurance programmes (NCRP, 2011). Radiation dose also needs to be measured and documented so that proper radiation management measures can be taken. These measures include patient follow-up for possible radiation injuries following high dose procedures (Miller et al., 2010).

Since intracranial aneurysm coil embolization is an interventional procedure, there is concern about high levels of radiation dose affecting the patients, especially the radiosensitive organs that are usually in, or close to, the radiation beam during these procedures. These organs include the skin, the thyroid gland and the eyes. The radiation effects on these organs include thyroid cancer, erythema on the skin and cataracts in the eyes (Shortt et al., 2007). Proper radiation dose management during intracranial aneurysm coil embolization is thus necessary to reduce the risk of possible radiation effects on these tissues. In the study described in this thesis, the radiation dose to the thyroid glands and skin of patients undergoing intracranial aneurysm coil embolization was measured using TLDs and KAP meters.

This chapter discusses interventional procedures with the focus on intracranial aneurysm coil embolization, the biological effects of radiation, radiation dosimetry, as well as methods of optimizing radiation exposure.

### **2.2. Interventional procedures**

Interventional procedures are fluoroscopically guided procedures that are often performed as an alternative to surgery for the treatment of certain pathologies, for example, aneurysms and biliary system obstruction (IAEA, 2010). Interventional procedures are among examinations that contribute the highest radiation doses to both patients and personnel, even though they are less frequently performed, compared to other radiological examinations.

Despite the high radiation doses, interventional procedures have some advantages over surgery. These advantages include the following (NCRP, 2011; Vaz, 2014):

- They are less invasive
- They result in reduced patient morbidity
- They also lead to reduced costs because of the shorter hospital stays

### **2.2.1. Intracranial aneurysms**

Intracranial aneurysms can rupture and cause subarachnoid haemorrhage. Aneurysmal SAH accounts for about 75% of all SAH. The most common type of intracranial aneurysms is the degenerative saccular aneurysm (Kowalczyk, 2014:126; Rodriguez-Regent et al., 2014).

There are two treatment options for intracranial aneurysms: endovascular coil embolization and surgical clipping of the aneurysm (Shortt et al., 2007). The results of major subarachnoid aneurysm trials, including the ISAT, the Clinical and Anatomic Results in the Treatment of Ruptured Intracranial Aneurysms (CLARITY) and the Barrow Ruptured Aneurysm Trial (BRAT), showed that patient morbidity and mortality at one-year follow-up after aneurysm treatment were better for coil embolization than for surgical clipping (Zhao et al., 2018). Li et al. (2012) found that surgical clipping leads to an increased risk of cerebral vasospasm and infarction compared to endovascular coiling of the aneurysm. However, there was no significant difference in the mortality rate following the two aneurysm treatment methods at one-year follow-up. Cerebral vasospasm and infarction are the major causes of fatality among patients with ruptured cerebral aneurysms (Li et al., 2012). The results of these studies favoured endovascular coil embolization and, as such, coil embolization has become the preferred method for treating intracranial aneurysms (Zhao et al., 2018).

During intracranial aneurysm coil embolization, fluoroscopy is used to guide the catheter to the intracranial artery of interest. Once the catheter is in the desired position, angiographic images of the cerebral arteries are acquired and embolization coils are deployed in the aneurysm. The cerebral angiographic images in Figure 2.1 show an intracranial aneurysm before and after coil embolization. The thyroid gland, the eyes, and the skin on the face, the neck and the scalp are exposed to radiation during this procedure. The radiation doses during intracranial coil embolization procedures can be high enough to cause early transient erythema and epilation (Suzuki et al., 2008).

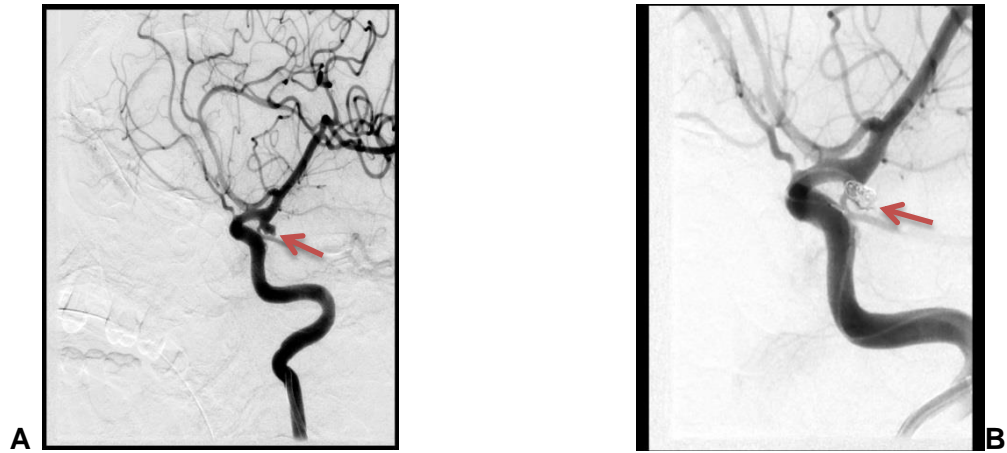


**Figure 2.1: Digital subtraction cerebral angiography showing a posterior communicating artery aneurysm (red arrows): A: before coil embolization; and B: post coil embolization (Images acquired as part of the study at the research site)**

### **2.3. Biological effects of radiation**

X-rays have a harmful effect on the human body as a result of ionization of atoms caused by the deposition of radiation energy on the tissues falling within the radiation beam. Ionization occurs when the energy of the radiation is high enough to cause ejection of the electron from the atom; and such radiation is called “ionizing radiation” (Hall, 2012:3). The absorption of this deposited energy can lead to injury to the tissues. It is primarily the effect of radiation on the deoxyribonucleic acid (DNA) that leads to biological effects of radiation. These biological effects can take one of the following forms:

- Cell death which can be observed hours to days after irradiation,
- Oncogenic effects with the cancer induction occurring years after exposure,
- Mutation of germ cells with the consequence of hereditary effects which may only occur after many generations.

(Hall, 2012:9-10).

Although biological effects of radiation were not the focus of the current study, it is important to understand that they can occur following exposure to radiation during intracranial aneurysm coil embolization. As suggested by Hall (2012:9-10) the skin exposed to radiation during intracranial aneurysm coil embolization is at risk of developing cell death, while the thyroid gland can develop late oncogenic effects.

### **2.3.1. Stochastic effects**

Stochastic effects are radiation effects which do not have a threshold dose below which they do not occur or above which they are sure to occur. They occur by chance and the chances of occurrence of stochastic effects increase with the increase in radiation dose. Stochastic effects are also termed 'late effects', as they are only seen years after the radiation exposure. Children have a higher risk of developing stochastic effects compared to adults because of higher tissue sensitivity and longer life expectancy. Cancer induction is an example of a stochastic effect (NCRP, 2011; Muhammad et al., 2017). Radiation doses used in diagnostic radiology are associated with stochastic effects except for interventional procedures, which can lead to both stochastic and deterministic effects (Hall, 2012).

### **2.3.2. Radiation effects to the thyroid gland**

The thyroid gland is mainly exposed to scatter radiation during intracranial aneurysm coil embolization (Shortt et al., 2007). The thyroid gland is more radiosensitive compared to other organs that are exposed to radiation during intracranial aneurysm coil embolization. The sensitivity of a tissue or organ towards radiation is indicated by a tissue weighting factor and the sum of all tissue weighting factors for the whole body is 1. The tissue weighting factor for the thyroid gland is 0.04 while the brain, the salivary glands and the skin have a tissue weighting factor of 0.01 respectively (ICRP, 2007).

Radiation exposure to the thyroid gland is associated with thyroid cancer induction, especially in children (Shortt et al., 2007). Radiation doses as low as 50–100 mGy have been reported to result in an increased risk of thyroid cancer in children (Sinnott et al., 2010). Richardson (2009) conducted a study to determine the association between radiation dose and thyroid cancer among atomic bomb survivors who were adults at the time of exposure. The study reported a positive association between thyroid radiation dose and thyroid cancer in women. Thyroid cancer was found in 241 females and 55 males who were over the age of 20 years at the time of exposure. Sinnott et al. (2010) also reported a small but significant thyroid cancer risk in females who were older than 20 years of age at the time of radiation exposure during the explosion of the atomic bomb in Japan. This thyroid cancer risk was not observed in male atomic bomb survivors. The radiation exposures during the atomic bomb explosion in Japan were between 5 and 150 mSv (Sinnott et al., 2010). The aforementioned studies indicate that females are at a higher risk of developing thyroid cancer than males. Other effects of radiation on the

thyroid gland, in adults, are hypothyroidism, hyperthyroidism and benign thyroid nodules (Sinnott et al., 2010; ICRP, 2012).

In a study by Theodorakou and Horrocks (2003), the mean thyroid dose to patients during cerebral embolization was 24 mSv and the maximum thyroid dose was 180 mSv. However, the thyroid doses to patients during intracranial aneurysm coiling reported by Shortt et al. (2007) were lower than this, with the mean thyroid dose of 8.29 mSv and the maximum thyroid dose of 21 mSv. Lunelli et al. (2013) reported a mean thyroid dose of 6.3 mGy and the maximum thyroid dose of 79.5 mGy from cerebral angiographies. The thyroid doses reported by Theodorakou and Horrocks (2003) are higher than the radiation exposure of between 5 and 150 mSv reported after the atomic bomb explosion in Japan.

### **2.3.3. Deterministic effects**

Deterministic effects have a minimum dose above which they occur, and the severity of the effect increases with an increase in the radiation dose. There are different threshold doses for different tissues and different effects. Examples of deterministic effects include skin burns, epilation and cataracts in the eyes (Muhammad et al., 2017). Although rare, deterministic effects can occur following complex interventional procedures (NCRP, 2011).

### **2.3.4. Radiation effects on the skin**

The skin on the face and the scalp are exposed to radiation during intracranial aneurysm embolization. Radiation effects on the skin are deterministic in nature therefore their severity depends on the delivered radiation dose (Miller et al., 2010). Table 2.1 lists the deterministic effects of radiation and the threshold doses above which they can occur.

**Table 2.1: Radiation effects on the skin (ICRP, 2012)**

Deterministic effect	Threshold dose	Time of onset
<b>Early transient erythema</b>	2 Gray (Gy)	2 to 24 hours
<b>Main erythema reaction</b>	6 Gy	1.5 weeks
<b>Temporary epilation</b>	3 Gy	3 weeks
<b>Permanent epilation</b>	7 Gy	3 week
<b>Dry desquamation</b>	14 Gy	4 to 6 weeks
<b>Moist desquamation</b>	18 Gy	4 weeks
<b>Late erythema</b>	15 Gy	8 to 10 weeks
<b>Ischaemic dermal necrosis</b>	18 Gy	After 10 weeks
<b>Dermal atrophy (1st phase)</b>	10 Gy	After 52 weeks
<b>Telangiectasis</b>	10 Gy	After 52 week
<b>Dermal necrosis (delayed)</b>	More than 15 Gy	After 52 weeks

D'Ercole et al. (2007) suggested threshold KAP values for deterministic effects of radiation on the skin. These threshold KAP values are listed in Table 2.2.

**Table 2.2: KAP threshold values for radiation effects on the skin (D'Ercole et al., 2007)**

Deterministic effect	KAP threshold value (Gy.cm <sup>2</sup> )
<b>Early transient erythema</b>	700
<b>Main erythema</b>	2,100
<b>Temporary epilation</b>	1,100
<b>Permanent epilation</b>	2,400

Suzuki et al. (2008) conducted a research study to determine the entrance skin dose from neuro-embolization procedures. In their study, the maximum entrance skin dose was more than 3 Gy in 20 out of 103 patients; more than 5 Gy in 2 patients; and epilation was seen in 6 patients. In a study conducted by Sandborg et al. (2012) to estimate the organ doses received during treatment for aneurysmal haemorrhage, 28% of patients exceeded the 3 Gy threshold dose for epilation and 6% of patients received a skin dose of more than 7 Gy. Theodorakou and Horrocks (2003) conducted a study to assess radiation dose to patients during cerebral embolizations. The threshold dose for early transient erythema (2 Gy) was exceeded in one patient, while the threshold dose for temporary epilation (3 Gy) was exceeded in another patient. A study performed by Sandborg et al. (2010) to determine the local skin and eye lens equivalent dose in interventional neuroradiology found the average skin dose to be 0.72 Sievert (Sv), while the maximum skin dose was 3 Sv.

The above-mentioned studies highlight the potential for the threshold doses for deterministic effects of radiation, particularly early transient erythema and temporary epilation, to be exceeded during neuro-interventional procedures. This raised concern about the possibility of skin injuries and, in turn, stimulated an interest amongst the researchers of the current study to assess radiation dose levels for similar procedures at the research site.

#### **2.4. Radiation dosimetry**

Radiation dosimetry plays an important role in radiation protection in diagnostic radiology (Muhammad et al., 2017). Radiation dose can be measured directly using TLDs, indirectly using KAP meters, or calculated using the x-ray tube kilovoltage (kV), tube current and exposure time product (mAs) and the FSD (Allisy-Roberts & Williams, 2008:45). Other dosimeters that can be used for direct measurements are ionization chambers and film dosimeters. Ionization chambers are more precise and accurate than TLDs, and can be read out directly, but their size can obscure areas of interest, making them unsuitable for use in patient dose measurements (International Commission on Radiation Units and Measurements, ICRU, 2005). In the current study, the absorbed doses to the thyroid gland were measured using TLDs while a KAP meter was used to determine the radiation dose to the skin. Dosimetric quantities used in the assessment of radiation dose to patients are absorbed dose, equivalent dose and effective dose (Hall, 2012:255-256).



### 2.4.1. Absorbed dose

Absorbed dose refers to the amount of energy absorbed from the ionizing radiation exposure per unit mass of an organ or tissue. The absorbed dose is measured in Gy and can be used as an indicator for the possibility of stochastic effects or deterministic effects on organs and tissues. For stochastic effects, the average absorbed dose over the organ or tissue is used. To determine the deterministic probability, the absorbed dose over the most irradiated portion of the tissue (for example, entrance skin) is used (ICRP, 2007).

### 2.4.2. Equivalent dose

Different types of radiations (e.g., x-rays, gamma rays, neutrons) result in different biological effects on the exposed tissue. The equivalent dose is the dose quantity that is used to determine radiation dose, taking the type of radiation into account (Muhammad et al., 2017). Equivalent dose is calculated for individual organs or tissues by multiplying the radiation weighting factor ( $W_R$ ) by the absorbed dose in that organ ( $D_T$ ), as in Equation 1.

$$H_T = W_R \times D_T \text{ (Equation 1) (IAEA, 2007).}$$

Radiation weighting factors for different kinds of radiations are listed in Table 2.3. As can be seen in this table, the radiation weighting factor for x-rays is 1, therefore the absorbed dose and the equivalent dose have the same numerical value for x-rays, although the equivalent dose is measured in the units of Sieverts to express the biological response (Bushberg et al., 2012:384; Muhammad et al., 2017).

**Table 2.3: Radiation weighting factors (ICRP 103, 2007)**

Radiation type	Radiation weighting factor ( $W_R$ )
Photons (x-rays and gamma rays)	1
Electrons	1
Protons	2
Alpha particles	20

Radiation exposure can result in different radiation effects in different tissues and organs, even for the same exposure, because of the difference in the radiosensitivity of tissues. To assess the

stochastic risk in organs due to the equivalent dose, a tissue weighting factor is applied to the equivalent dose for each organ. The sum of all tissue weighted equivalent doses is the effective dose (ICRP, 2007). The tissue weighting factors, according to ICRP (2007), are listed in Table 2.4.

**Table 2.4: Tissue weighting factors (ICRP 103, 2007)**

Tissue	Weighting factor ( $W_T$ )
<b>Bone-marrow (red), colon, lung, stomach, breast</b>	0.12
<b>Gonads</b>	0.08
<b>Bladder, oesophagus, liver, thyroid</b>	0.04
<b>Bone surface, brain, salivary glands, skin</b>	0.01

### 2.4.3. Thermoluminescent dosimeters

Thermoluminescence is a process whereby a material absorbs energy (for example, radiation from ionizing radiation exposure) and re-emits that energy in the form of light, following heating. During irradiation, some electrons are raised from the valence band to the conduction band where they get trapped in the defects or impurities of the phosphor material. When heat is applied, these electrons are freed from the traps and they release the energy in the form of light as they return to the valence band. The amount of light emitted is proportional to the radiation dose absorbed by the thermoluminescent material. TLDs operate in this manner (Allisy-Roberts & Williams, 2008:20; Bhatt & Kulkarni, 2014).

TLDs have the following advantages (IAEA, 2007; Bhatt & Kulkarni, 2014):

- They measure the total radiation dose accumulated over the period of exposure.
- They are small, and therefore can be placed anywhere on the patient without obscuring the area of interest.

- They are re-usable.
- They are sensitive to a wide range of photon energies.
- They have low thermo luminescence fading. Fading is a process by which the electrons that were trapped during irradiation are slowly released at room temperatures.

TLDs are sensitive to dirt, grease and light; therefore, special care should be taken when handling them. To protect against dirt and grease, TLDs are handled using special prongs with Teflon tips or vacuum tweezers; and they should be encapsulated before use (ICRU, 2005).

Thermoluminescent dosimeters are made of different phosphor materials which include lithium fluoride, lithium tetraborate, magnesium borate and calcium fluoride. Lithium fluoride doped in magnesium (Mg) and titanium (Ti) (LiF:Mg,Ti) has desirable properties of thermo-luminescence due to the presence of natural impurities, magnesium and titanium, that act as trapping centres (Bhatt & Kulkarni, 2014). LiF:Mg,Ti TLDs, also known as TLD-100, are nearly tissue equivalent which makes them suitable for medical dosimetry; and, for this reason, they are most widely used (Furetta, 2003:426). Lithium fluoride TLDs have a relatively low fading of about 5% per year. They are also useful to a wide dose range of between 20 $\mu$ Gy and 10Gy (Bhatt & Kulkarni, 2014; Fernández et al., 2016). However, LiF TLDs have a disadvantage of low sensitivity, especially at low energies, compared to TLDs with higher atomic numbers, like calcium sulphate (CaSO<sub>4</sub>) (Furetta, 2003:39) and this. LiF:Mg,Ti TLD chips were used for the current study because of the advantages listed above. However, the low sensitivity of LiF TLDs at low energies could affect the accuracy of TLD readings in the current study especially in cases where only scatter radiation was measured.

#### **2.4.3.1. TLD calibration**

TLDs have an unstable response to radiation exposure. As a result, there is a degree of uncertainty in the TLD measurements. To determine their response to a certain energy level (tube voltage) and ensure correct measurements, they are calibrated against a measuring instrument of known, reliable standard that has been calibrated. An ionization chamber is recommended for TLD calibration because of its good long-term stability and small variation of response with varying energy (IAEA, 2007). Both the reference dosimeter and the dosimeter under calibration should be exposed to the same x-ray quality during calibration (ICRU, 2005)

Calibration is performed using the same x-ray beam quality which the TLDs will be exposed to during patient dosimetry (Fernández, et al. 2016). The quality of the x-ray beam is determined by

the x-ray tube voltage, the half value layer (HVL) and the total filtration used. The IAEA (2007) and ICRU (2005) recommend a tube voltage of  $\pm 80$  kV with a total filtration of 3 mm Al and an incident air-kerma of 5 – 10 mGy for calibration of TLDs to be used in diagnostic radiology dosimetry. Calibration using a free in air geometry is recommended to limit the effect of backscatter on the dose measurements; and a sufficient number of readings must be performed to reduce the standard deviations of mean values and ensure reliable results (IAEA, 2007). The calibration method described above was employed during the current study.

#### **2.4.3.2. TLD read out and annealing**

Following irradiation, the TLDs are heated to emit light which is then measured to determine the radiation dose that was absorbed during radiation exposure (Allisy-Roberts & Williams, 2008:20). To ensure reliable results, TLDs need to be read out and annealed carefully (ICRU, 2005). The heating process is performed in pure nitrogen to suppress oxidation that could result in thermoluminescent material contamination (Furetta, 2003).

There are three steps in the TLD heating process, namely the pre-readout annealing, the readout phase, and the post-readout annealing. Annealing is the heating process that is performed to erase all residual traps or radiation history in the TLD to increase the accuracy (Furetta, 2003:9). The pre-readout annealing, also termed the 'post irradiation anneal', is performed after the TLD irradiation to remove all low temperature signals before reading. This process reduces fading which could result in inaccurate readings. A pre-read annealing of 10 minutes at 100°C in the oven is recommended for LiF:Mg,Ti TLDs (Furetta, 2003:17; Bhuiyan et al., 2007). The post reading or pre-irradiation annealing removes all the residual traps in the TLD, i.e., the TLD is reset to zero before it is re-used (Furetta, 2003:10). Annealing is performed in the annealing oven. It is suggested that the process can also be performed in the TLD reader for doses lower than 10 mGy. The recommended post-reading annealing process in the TLD reader for LiF:Mg,Ti TLDs is 30 seconds at 300–400°C. In the oven, the post-reading annealing process for LiF:Mg,Ti TLD is 1 hour at 400°C, followed by 2 hours at 100°C, or 20 hours at 80°C, after which the TLDs are kept at room temperatures for 1 hour for cooling purposes (Furetta, 2003:15).

The TLDs used for the current study were annealed in the annealing oven for 1 hour at 400°C followed by 2 hours at 100°C, then left overnight for cooling.

#### **2.4.4. Air-kerma area product meter**

Dose area product meters or 'air-kerma area product meters' are parallel plate ionization chambers that are attached to the collimator of the x-ray tube. It measures the total radiation dose over the x-ray beam area, and thus the total radiation dose delivered to the patient during the entire procedure. The standard unit of measurement is Gy.cm<sup>2</sup>. The KAP reading is documented and reset to zero after every patient. According to the Food and Drug Administration (FDA) requirement, all fixed fluoroscopy units installed after 2006 must have a fixed KAP meter with a display unit attached (Bushberg et al., 2012:306). In South Africa, all fixed fluoroscopy units, including those that were already installed, had to have KAP meters by January 2008 (South Africa, Department of Health Directorate: Radiation Control, 2012).

KAP meters are associated with an error of between 30% and 40% for skin dose estimation (McParland, 1998; Miller et al., 2003; D'Ercole et al., 2007). According to the IAEA (2007), the KAP error should be limited to within 25%. Like TLDs, KAP meters need to be calibrated to increase their accuracy. The calibration factors determined during KAP calibrations are recommended for dose correction and thus reduction of the uncertainty error to within 25% (IAEA, 2007). KAP meter calibrations should be performed on acceptance and yearly thereafter, according to the manufacturer's specifications (South Africa, Department of Health Directorate: Radiation Control, 2012). The KAP meter employed during the current study underwent annual calibrations according to the manufacturer's specifications.

#### **2.4.5. Skin dose assessment**

As a result of the potential for interventional procedures to cause radiation skin injuries, it is crucial for the maximum skin dose to the patients to be assessed (IAEA, 2010). The dose metrics that can be used to estimate patient dose in fluoroscopy are fluoroscopy time, peak or maximum skin dose, reference dose and KAP. Maximum skin dose (MSD) is the preferred dose metric to estimate the deterministic risk to the patients. However, MSD is difficult to measure, especially for interventional procedures with multiple fluoroscopic and radiographic projections. Also, many fluoroscopic units do not have the functionality to display MSD (Jaco & Miller, 2010). In the absence of MSD information, KAP is the recommended quantity for patient skin dose assessment in fluoroscopy (IAEA, 2007; Allisy-Roberts & Williams, 2008:45) because KAP correlates reasonably well with MSD, according to Jaco and Miller (2010).

KAP can accurately estimate MSD when the x-ray tube angulation, the distance of the table and image intensifier from the tube, and the size of the collimated field are known throughout the procedure. However, changes in the above geometries can lead to an error of about 30–40% in MSD readings and there is generally poor correlation between MSD and KAP (Miller et al., 2003). Despite the argument posed by Miller et al. (2003), previous studies found good agreement between KAP and maximum skin dose for neuro-interventional procedures (Theodorakou & Horrocks, 2003; D’Ercole et al., 2007; IAEA, 2010; Sandborg et al., 2010).

Bor et al. (2004) and Acton et al. (2018) warn that KAP does not provide information about the most irradiated areas on the skin and therefore is not suitable for estimating the deterministic risk to the patients. Jaco and Miller (2010) recommend that all patients that are exposed to KAP values of 500 Gy.cm<sup>2</sup> should be followed up for possible skin injuries.

TLDs give a better estimation of entrance skin dose as well as the deterministic risk (Bor et al., 2004). However, the use of TLDs for skin dose measurements is limited because it is often not possible to know the area of highest skin dose beforehand, especially in procedures involving various projections (Balter et al., 2002). A large number of TLDs spread over the exposed part of the body would be required to overcome this problem but it is difficult to manage large numbers of TLDs. Another limitation of using TLDs is that they do not provide real-time dose display. The radiation dose information is only available after the procedure once the TLDs have been read (Balter et al., 2002; IAEA, 2010). Radiochromic films also provide a good estimation of entrance skin dose, however, like TLDs, there is no real time dose display. An advantage of radiochromic film over TLDs is that it covers a large area and can provide information on the dose distribution over the exposed area (D’Ercole et al., 2007).

In a study by Theodorakou and Horrocks (2003), the entrance skin dose was measured using TLDs and the DAP values were also recorded during cerebral embolizations. The TLD entrance skin dose ranged between 0.4 Gy and 3.4 Gy. The mean DAP value was 53 Gy.cm<sup>2</sup> and the maximum value was 321 Gy.cm<sup>2</sup>. D’Ercole et al. (2007) conducted a study on the maximum skin dose in cerebral embolization procedures. Out of the 48 procedures included in their study, maximum skin dose was measured using radiochromic film in 21 procedures and calculated from DAP in 27 procedures. The MSD was found to range between 0.23 and 3.2 Gy with a mean of 1.16 Gy. A good correlation between DAP and maximum skin dose was also found in their study. Suzuki et al. (2008) found skin doses during neuro-embolization procedures to be between 0.4 Gy and 5.6 Gy with an average of 1.9 Gy. The average DAP value for their study

was 233 Gy.cm<sup>2</sup>. Sandborg et al. (2010) reported on TLD measured skin doses and KAP values for cerebral aneurysm coiling. In their study, the average TLD measured skin dose was 0.72 Sv and the maximum TLD skin dose was 3 Sv. The mean KAP value was 121 Gy.cm<sup>2</sup> and the maximum KAP was 436 Gy.cm<sup>2</sup>. Ihn et al. (2016) reported average KAP values of 218 Gy.cm<sup>2</sup> for cerebral aneurysm coiling. Acton et al. (2018) found mean and maximum KAP values during cerebral aneurysm embolization to be 108 Gy.cm<sup>2</sup> and 366 Gy.cm<sup>2</sup> respectively. The mean KAP values from therapeutic neuroradiology procedures reported by Bor et al. (2005) and Rampado and Ropolo (2005) were 215.7 Gy.cm<sup>2</sup> and 191.7 Gy.cm<sup>2</sup> respectively.

The afore-mentioned studies indicate that the maximum skin dose threshold value of 2 Gy can be exceeded during cerebral embolization studies, while the KAP action value of 500 Gy.cm<sup>2</sup> for patient follow-up was not reached in all studies.

In the present study, KAP as well as maximum entrance skin dose, when displayed by the angiography unit, were used to determine the maximum skin dose.

#### **2.4.6. Monte Carlo calculations**

Radiation dose can be measured using dosimeters or calculated using the Monte Carlo method. The Monte Carlo program is computer-based software that is used to calculate organ doses received from x-ray exposure. Monte Carlo organ dose calculations play an important part in patient dosimetry as measuring organ doses often involves experimental measurements in phantoms, which can be difficult and time consuming. The Monte Carlo method simulates, on computational hermaphrodite phantoms that represent human beings, the interaction of x-ray photons with tissues (Tapiovaara & Siiskonen, 2008). The most probable photon interactions at diagnostic radiology kV range are the photoelectric absorption and Compton effect (Allisy-Roberts & Williams, 2008: 14). The energy deposition in each tissue or organ is calculated and stored in order to calculate the radiation dose in these organs. The number of simulated photon interactions in the organs or photon histories affects the accuracy of the dose estimation. A large number of photon interactions is required for improved accuracy (Tapiovaara & Siiskonen, 2008). Peters (2017) found no difference in the radiation dose estimation resulting from 10 000, 50 000 and 100 000 photon histories.

A Personal Computer program for x-ray Monte Carlo (PCXMC) was used in this study to calculate the thyroid gland and skin doses received by patients during intracranial aneurysm coil embolization. The radiation field size, the x-ray beam angulation, the FSD, the x-ray beam

spectrum and KAP or entrance air-kerma values are required to calculate the organ doses and effective doses in PCXMC. The maximum kV that can be used in PCXMC is 150. The accuracy of the calculated dose is dependent on the accuracy of the anatomical model used to represent the actual patients as well as the radiation field size. For effective dose calculations, ICRP 103 and ICRP 60 recommended tissue weighting factors are also used (Tapiovaara & Siiskonen, 2008).

## **2.5. Justification and optimization of dose**

For high radiation dose procedures especially, adherence to radiation protection measures is vital. Such measures are guided by the two principles of radiation protection in medicine, namely justification of exposure and optimization of protection. The principle of justification means that the radiation exposure should only be carried out when there is sufficient benefit to the patient. Optimization of protection entails ensuring that, for justified procedures, the radiation exposure is optimised so as to maximise the benefit to the patients while keeping the radiation risks low (ICRP, 2007). The importance of applying justification and optimization principles is also emphasized by the South African Radiation Control Directorate (South Africa, Department of Health Directorate: Radiation Control, 2015).

Optimization can be achieved by applying the ALARA principle – using the lowest possible radiation exposure to produce a clinically acceptable diagnostic image quality (Trapp & Kron, 2008:103). In clinical practice, the NRC (2011) indicates that achieving the ALARA principle during interventional procedures can be achieved by:

- Using low fluoroscopy mode, as this leads to a decreased radiation dose without impairing the image quality, compared to normal fluoroscopy mode.
- Collimating to the required field of view to reduce scatter radiation and increase image quality.
- Increasing the distance between the x-ray tube and the patient.
- Limiting use of electronic magnification and steep angulations of the C-arm (>30° left or right and >15° cranially) as these result in increased radiation doses.
- Acquiring DSA images only when high image quality is necessary, with the lowest possible frame rate.



These strategies for radiation dose optimization are applied at the research site during intracranial aneurysm embolization procedures. The use of magnification and steep angulation of the C-arm are excluded as these are often desirable during the deployment of the coil.

The C-arm angulation is determined by the aneurysm location and shape. The view that best shows the aneurysm in its entirety is used. Similarly, a magnified view ensures that the aneurysm can be well seen.

Another method of applying the optimization principle is by employing DRLs. One of the themes at the co-hosted Society of Radiographers of South Africa (SORSA) and the Radiological Society of South Africa (RSSA) 2017 congress in Durban, South Africa, was radiation justification and optimization. In view of the limited DRLs in South Africa, the take home message from this congress was for institutions to start developing DRLs for the most common radiological procedures. This implies that the application of dose optimisation in the form of DRLs in South Africa is encouraged by these two professional associations. One of the aims of this study was to establish DRLs for aneurysm coil embolization procedures.

## **2.6. Diagnostic reference levels**

Diagnostic reference levels were introduced by the ICRP in 1996 for diagnostic radiology and nuclear medicine procedures with the following aims (ICRP, 2001):

- To identify and reduce the number of unjustified high dose values.
- To promote good practice for specific imaging tasks and clinical indications.
- To promote an optimum range of values for specified medical imaging protocols.

A DRL is a radiation dose management tool that can be used as a reference against which patient doses are compared to identify unusually high levels of radiation dose. If the patient doses are found consistently to exceed the DRLs for a certain procedure, the equipment and that procedure should be investigated with the aim of reducing the radiation dose and minimising the risk for stochastic effects (ICRP, 2017).

Diagnostic reference levels for adults are usually defined for an average-sized person, typically between 70kg and 80kg, and are set at a 75% (third quartile) level of the dose to those patients (Trapp & Kron, 2008:108). However, when setting DRLs for intracranial aneurysm coiling, it is not necessary to take the patients' weight into consideration as all human heads are, on average, the same size and there was no difference in DRLs for cerebral angiography between

the group in which the body weight of patients was considered and the group where the body weight was not considered (Miller et al., 2009). The IAEA (2010) also suggest that the radiation dose in interventional procedures is more dependent on the procedure complexity than patient weight.

The radiation dose parameter to be used for a DRL depends on the type of examination. For fluoroscopic procedures, the parameter used is the DAP (Trapp & Kron, 2008:109). The ICRP (2017) suggests including the number of acquired images or frames, fluoroscopy time and cumulative dose, if available, when setting DRLs for interventional procedures. The ICRP (2017) argue that including the above parameters would make it easy to identify the reasons for high radiation doses, should they occur. Fluoroscopically guided interventional procedures have a wide variety of patient doses due to the differences in duration and complexity of each procedure (ICRP, 2017).

Bogaert et al. (2009) conducted a study to determine DAP action levels and DRLs in interventional cardiology, taking into account the procedure complexity. These authors classified the complexity of the procedures as 'easy', 'normal' or 'difficult' based on the duration of the procedure, the number of lesions and the accessibility of the coronary arteries. The results of their study indicated that the complexity of the procedure was the main factor that affected the radiation dose. The radiation dose for normal and difficult procedures was significantly higher than the dose for easy procedures.

In another study by D'Ercole et al. (2012) to determine local diagnostic reference levels for cerebral angiography and cerebral embolizations, the complexity of the study was defined according to the aneurysm location and the aneurysm size. The results of this study by D'Ercole et al. (2012) showed no significant difference in DRLs between procedures deemed easy and those deemed complex according to the aneurysm location. There was, however, a significant increase in DRLs for embolization of large aneurysms compared to small aneurysms.

The above-mentioned studies demonstrate the necessity of taking the relative complexity of the procedure into consideration when setting DRLs for interventional procedures. However, according to the ICRP (2017), that would require large amounts of data which may not always be possible to get. The complexity of the procedure was not considered when setting DRLs for the current study as the sample size was not large enough to allow for the complexity of the

study to be considered. The third quartiles of the KAP values, the fluoroscopy time and the number of image frames were used to establish DRLs in the current study.

### 2.6.1. Published DRLs for intracranial aneurysm coiling procedures

Studies have been conducted in different parts of the world to determine the DRLs for intracranial aneurysm coiling, among other procedures. The results of some of these studies are summarized in Table 2.5.

**Table 2.5: A summary of published DRLs for intracranial aneurysm coiling**

Author/Year of publication	Country	Sample size	Fluoroscopy time (min.) (3 <sup>rd</sup> quartile)	No. of image frames (3 <sup>rd</sup> quartile)	DAP range (Gy.cm <sup>2</sup> )	DRL (Gy.cm <sup>2</sup> ) (3 <sup>rd</sup> quartile)
<b>Verdun et al., 2005</b>	Switzerland	58	Not available	Not available	24.0 – 1345.0	352.0
<b>Aroua et al., 2007</b>	Switzerland	58	3.3–134.0 (range)	60.0-3348.0 (range)	24.0 – 1345.0	440.0
<b>Miller et al., 2009</b>	United States of America	148	90.0	1350	67.8 – 825.15	339.4
<b>Sandborg et al., 2010</b>	Sweden	226	7–189 (range)	Not available	121.0 – 436.0	157.0
<b>D’Ercole et al., 2012</b>	Italy	72	46.15	664.75	120.9 – 940.4	486.11
<b>Söderman et al., 2013</b>	Sweden	38	16.0	845	8.0 – 635.0	196.0
<b>Erskine et al., 2014</b>	Australia	91	32.0	Not available	Not available	152.9
<b>Chun et al., 2014</b>	Korea	111	61.0	241 ± 92 (mean)	Not available	272.8
<b>Ihn et al., 2016</b>	Korea	371	64.7	567.3	20.0 – 1154.4	271.0

Table 2.5 shows a wide variation in DRLs between the different studies. This variation could be attributable to a number of factors including different complexity of the procedures, experience of the interventionalists, equipment age, different dose reduction technologies on equipment and different imaging techniques and protocols at different hospitals (Acton et al., 2018).

D'Ercole et al. (2012) and Aroua et al. (2007) reported the highest DRL values of 486 and 440 Gy.cm<sup>2</sup> respectively for cerebral embolizations. D'Ercole et al. (2012) cited different filtration and no dose optimization in radiography mode and the use of continuous instead of pulsed fluoroscopy mode as the possible causes for the high DAP values in their study.

Söderman et al. (2013) performed dose measurements during diagnostic cerebral angiographies and interventional neuroprocedures using the same angiography equipment before and after it was fitted with an advanced image noise reduction algorithm. The DAP values for interventional procedures without the image noise reduction technology ranged from 28 – 1114 with the third quartile of 518 Gy.cm<sup>2</sup>. Following the image noise reduction technology installation, the DAP values were reduced to between 8 and 635 Gy.cm<sup>2</sup> with the 3<sup>rd</sup> quartile value of 196 Gy.cm<sup>2</sup>.

### **2.6.2. DRLs in South Africa**

A literature review that was conducted by Meyer et al. (2017) to review published DRLs in lower- and middle-income countries found that only six African countries had published twenty publications related to DRLs i.e. Ethiopia, Kenya, Nigeria, Tunisia, Sudan and South Africa. Only two out of twenty publications were on DRLs for interventional procedures and these were both from Kenya. According to Meyer et al. (2017) only two publications related to DRLs were from South Africa, and these were Engel-Hills and Hering's (2001) study on DRLs for barium enema examinations and Nyathi's (2009) study on dose audits for radiography examinations.

In line with the ICRP recommendations, the Radiation Control Directorate of the Department of Health of South Africa gave a directive for the development of DRLs for all radiographic and fluoroscopic procedures (South Africa, Department of Health Directorate: Radiation Control, 2015:14). As far as could be established, there are limited studies that were performed to determine DRLs for fluoroscopy and fluoroscopically guided procedures in South Africa. These will be discussed in the next section.

### **2.6.2.1 DRLs for fluoroscopy procedures in South Africa**

Engel-Hills and Hering (2001) conducted a study to determine the typical doses received by patients during barium enema studies. A DAP meter was used for dose measurements and the third quartile of the DAP readings, 84 Gy.cm<sup>2</sup>, was proposed as the initial DRL for South Africa.

Nabasenja (2009) determined radiation doses for barium meals and barium enemas at three hospitals in the Western Cape, South Africa. The radiation doses were measured using DAP meters and the third quartile DAP values were 20.1 Gy.cm<sup>2</sup> for barium meals and 36.5 Gy.cm<sup>2</sup> for barium enemas.

Nyathi (2012) performed a dose audit for fluoroscopic and radiographic procedures. The DAP meter was used to determine skin dose and dose area product for fluoroscopic examinations which included barium swallow, barium meal, barium enema, cystourethrogram, fistulogram, myelogram, nephrostomy and loopogram. The DRLs from the afore-mentioned study were 24.7 Gy.cm<sup>2</sup> for barium swallow, 26.5 Gy.cm<sup>2</sup> for barium meal and 68.4 Gy.cm<sup>2</sup> for barium enema. For cystourethrogram, fistulogram, myelogram and nephrostomy, the DRLs were 18.6 Gy.cm<sup>2</sup>, 20.6 Gy.cm<sup>2</sup>, 34 Gy.cm<sup>2</sup> and 20.7 Gy.cm<sup>2</sup> respectively.

Peters (2017) conducted a study to determine effective dose and entrance skin dose from dose area product values for barium studies. The 75<sup>th</sup> percentile of the DAP readings was used to determine the DRLs for these procedures. The proposed DRLs were 12.8 Gy.cm<sup>2</sup>, 17.4 Gy.cm<sup>2</sup> and 16 Gy.cm<sup>2</sup> for barium swallow, barium meal and barium enema respectively. Effective dose and entrance skin doses for the above study were computed using a Monte Carlo software program.

The above studies suggest that there has been a significant improvement in dose optimization for barium enema studies in South Africa, with DRLs decreasing from 84 Gy.cm<sup>2</sup> in 2001 to 16 Gy.cm<sup>2</sup> in 2017. However, there is not much difference in radiation doses for barium meal studies with DRLs of 20.1 Gy.cm<sup>2</sup> in 2009 and 17.4 Gy.cm<sup>2</sup> in 2017.

### **2.6.2.2. DRLs for angiography and interventional procedures in South Africa**

Muller (2014) performed a retrospective study to determine the patient radiation doses from diagnostic and interventional procedures between 2006 and 2009. The skin dose values were calculated from the DAP readings and presented in milligrays (mGy). The maximum skin dose received during diagnostic cerebral angiography was 470 mGy, with the majority of procedures

(257 out of 287) resulting in skin doses of between 150 and 180 mGy. The 75<sup>th</sup> percentile of dose for diagnostic cerebral angiography during the above-mentioned study was 173 mGy.

De Vos (2015) completed a Master's thesis on radiation dose optimization in interventional radiology and cardiology using diagnostic reference levels. The study included data from 24 procedures, including cerebral angiography and intervention, as well as coronary angiography and intervention in interventional radiology theatres at 27 private hospitals. The study focused on six cardiac procedures that were common at the research sites. The DRLs were established using the DAP readings. The mean DAP values for diagnostic cerebral angiography and cerebral interventions were 138.3 and 177.8 Gy.cm<sup>2</sup> respectively.

Makosa and Conradie (2015) conducted a study to determine DRLs for a variety of procedures including diagnostic and interventional cerebral angiography, barium studies, percutaneous transhepatic cholangiography and coronary angiography. DAP meter readings were used to determine DRLs and the proposed DRLs for diagnostic cerebral angiography and interventional cerebral angiography were 143 Gy.cm<sup>2</sup> and 200 Gy.cm<sup>2</sup> respectively.

## **2.7. Effect of the aneurysm location on radiation dose**

According to Acton et al. (2018), the aneurysm location has the biggest effect on the patient radiation dose during intracranial aneurysm coiling. During intracranial aneurysm coil embolization procedures, the x-ray tube angulation is determined by the aneurysm location and the view that best shows the aneurysm is used for guiding the catheter and embolization coils into the aneurysm. This sometimes necessitates the use of steep angulations of the x-ray tube which have been reported to lead to increased radiation doses to patients (NCRP, 2011). It is thus hypothesised that an aneurysm that requires the use of steep angulations during fluoroscopy and image acquisition would result in an increased radiation dose to the patient, compared to an aneurysm that requires use of a straight x-ray tube.

Aneurysms that are in difficult-to-reach areas may also result in an increased radiation dose to patients, as prolonged fluoroscopy would be required to place the catheter successfully in the aneurysm. Complex aneurysms also warrant additional image acquisitions to define clearly the aneurysm and its neck (Acton et al., 2018). In a study by Acton et al. (2018), the 75<sup>th</sup> percentile of DAP value for coiling of anterior circulation aneurysms was 98 Gy.cm<sup>2</sup>, while it was 151 Gy.cm<sup>2</sup> for posterior circulation aneurysms. These authors attributed the increased radiation dose for the coiling of posterior circulation aneurysms to the complex anatomy of these

aneurysms that sometimes requires assisted coiling. D'Ercole et al. (2012), however, assigned a complexity index of 0 to posterior circulation aneurysms and a complexity index of 1 to anterior circulation aneurysms, suggesting that these authors deemed posterior circulation aneurysm coiling to be less complex than anterior aneurysm coiling. The results of the study by D'Ercole (2012) showed no significant difference in the DRLs between anterior and posterior circulation aneurysms.

## **2.8. Conclusion**

The current study was aimed at establishing the average radiation dose received during intracranial aneurysm embolization, as well as DRLs for this procedure, at an academic hospital. This chapter has discussed literature related to radiation dose from intracranial aneurysm coil embolization procedures. The reviewed literature shows that deterministic effects of radiation can be observed following intracranial aneurysm coil embolization procedures. The use of DRLs as radiation dose optimization tools was discussed. The need for establishing DRLs at hospital level was identified, as there can be a wide variation in DRLs for intracranial aneurysm coiling. The reviewed literature further highlights the lack of published DRLs for these procedures in South Africa. The next chapter describes in detail the research methodology employed during the current study. Thereafter the findings relative to this study will be described in Chapter 4.

## **CHAPTER 3: RESEARCH METHODOLOGY**

This chapter explains the research question and objectives of the current study and describes the research methods employed to answer the research question. The research population and sampling as well as the inclusion and exclusion criteria for this study, are also discussed. The data collection and data analysis applied will also be explained.

### **3.1. Research question and objectives**

The research question for this study was: “What is the average radiation dose to patients undergoing intracranial aneurysm coil embolization?”

The research objectives of the study were to:

- i. Determine the radiation dose to patients’ thyroid glands using TLDs and skin by means of a KAP meter during intracranial aneurysm coil embolization.
- ii. Ascertain whether the anatomical location of the intracranial aneurysm affects the radiation dose to the patients.
- iii. Establish preliminary diagnostic reference levels for intracranial aneurysm coil embolization.
- iv. Compare measured thyroid gland and skin doses to thyroid gland and skin doses calculated using the PCXMC program.

### **3.2. Research methods**

This research study design consisted of three components. The first component was a quantitative, prospective study, which involved measurement of the radiation dose to patients undergoing intracranial aneurysm coil embolization, here referred to as actual coil embolization study. The second component entailed the measurement of radiation doses during the simulation of intracranial aneurysm coil embolization procedures on the phantom, here referred to as phantom based simulation study. The third component involved calculation of the thyroid gland and skin doses using the PCXMC program.

### **3.3. Research study site**

The research study was conducted in the angiography suite within the radiography department at a large tertiary academic hospital in Cape Town. All intracranial aneurysm coil embolization



procedures were performed using a Siemens Artis Zee biplane angiography unit manufactured in Germany.

### **3.4. Research population**

The population for this study included all adult patients with clinically confirmed intracranial aneurysms that were treated at the research site during the study period (January to November 2018).

#### **3.4.1. Inclusion criteria**

Patients with clinically confirmed intracranial aneurysms that required endovascular coil embolization were recruited for participation. Patients were of all genders and ethnic groups and were aged between 18 and 75 years.

#### **3.4.2. Exclusion criteria**

The following patients were excluded from the study:

- Children and psychiatric patients, as they were considered vulnerable participants for the purpose of this study.
- Patients with low levels of consciousness, as they were unable to give informed consent.
- Patients with extracranial aneurysms and patients referred for other intracranial embolization procedures, e.g., arterio-venous malformation and dural fistula embolizations.

#### **3.4.3. Sampling**

During the current study, a convenience sampling method was employed where all adult patients between the ages of 18 and 75 years who met the inclusion criteria were recruited to be part of the study. Convenience sampling is a quick non-probability sampling method which means that the required sample size can be obtained in a shorter period of time (Maree et al., 2016). For this reason, this sampling method was chosen for the current study. However, the samples obtained with convenience sampling may not be representative of the population (Maree et al., 2016).

#### **3.4.4. Sample size**

A total of 96 aneurysm coil embolization procedures were performed at the research site during the study period. Fifty-four patients were excluded for various reasons, including the following:

- Patients' refusal to participate in the research.
- Patients with low levels of consciousness.
- No access to the TLDs when the medical physicist was unavailable.
- Urgent cases that could not wait until the researcher arrived at the research site.

Of the 42 coiling procedures included in the research study, three were excluded due to errors in the TLD reading process. Another five were excluded because only one TLD was used on each patient. This resulted in a sample size of 34 patients, four of which were diagnostic studies only. The sample size of 34 was considered adequate, as Miller et al. (2009) suggest a minimum sample size of approximately 30 patients to achieve a confidence level of 95% when setting reference levels for interventional radiology procedures. The ICRP (2017) also recommends a minimum sample size of about 30 patients for setting DRLs for fluoroscopically guided procedures.

#### **3.5. Dose measurement materials**

Lithium fluoride TLD chips were used to measure the radiation dose to the thyroid gland during both the phantom and patient studies. In addition to using TLDs for dose measurements during intracranial aneurysm coil embolization on patients, the KAP meter was also used to determine the skin dose and the diagnostic reference levels for all procedures.

##### **3.5.1. Thermoluminescent dosimeters**

TLDs have to be calibrated before use to determine their response to a certain energy level (tube voltage) and to improve accuracy. The TLDs used for the current study were calibrated using the materials and procedure described below. To protect them from dirt and grease, TLDs were encapsulated in clear plastic before use. A Teflon<sup>TM</sup>-coated vacuum pen was also used for TLD handling before the TLDs were encapsulated in clear plastic.

###### **3.5.1.1. TLD calibration materials**

The following objects were used for TLD calibration:

- A Shimadzu general x-ray machine (Model UD 150L – 40E) with the half value layer of 1.5 mm aluminium (Al) at 70 kV. Routine quality control (QC) was performed on this equipment. The QC tests include annual kV repeatability and accuracy tests. The previous QC tests were performed two months before the calibration of TLDs for the purposes of this study.
- Thirteen encapsulated lithium fluoride TLDs of the same batch.
- A PTW – Freiburg 30 cm<sup>3</sup> cylindrical ionization chamber (Figure 3.1).
- A PTW UNIDOS electrometer.

The ionization chamber and the electrometer underwent routine quality assurance and calibration. The previous calibration was performed four months prior to the calibration for this study using the German National Laboratory standards (calibration certificates are attached as Appendix A).



**Figure 3.1: A PTW - Freiburg 30 cm<sup>3</sup> cylindrical ionization chamber.**

### **3.5.1.2. TLD calibration procedure**

The TLD calibration procedure recommended by IAEA (2007) for diagnostic radiology dosimetry was followed (Refer to 2.4.3.1.). Firstly, the 30 cm<sup>3</sup> cylindrical ionization chamber was mounted on the tripod stand and placed at a distance of 100 cm from the focus of the x-ray tube. Secondly, the ionization chamber was connected to the PTW UNIDOS electrometer for dose readings (Figure 3.2). A tube voltage of 70kV was used. The tube current and exposure time were set to deliver an air-kerma of 10 mGy. Thirdly, three x-ray exposures were performed to ensure reliability of readings, and the dose reading was documented after each exposure.

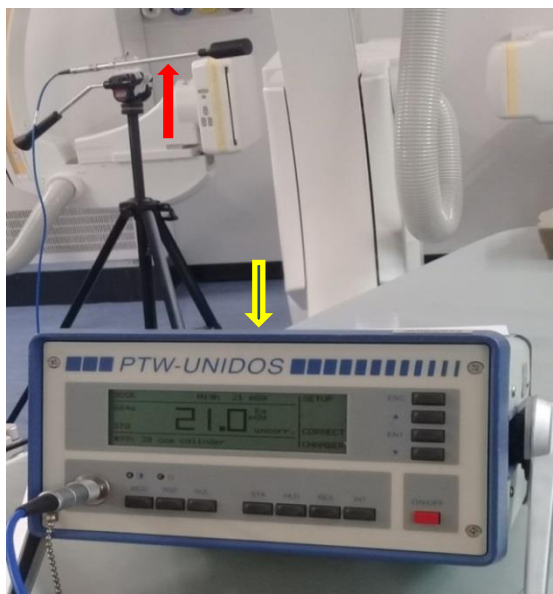


**Figure 3.2: A PTW Freiburg 30cm<sup>3</sup> cylindrical ionization chamber (red arrow) connected to a PTW-UNIDOS electrometer (yellow arrow) for calibration prior to commencement of the data collection (Images acquired by the researcher for this research purposes)**

Finally, the TLDs were exposed to radiation. Twelve encapsulated TLDs (bearing identification numbers) were placed on a 30 cm long polyethylene foam pad (Figure 3.3) which was then mounted on a tripod stand. The TLDs were exposed using the same exposure parameters as for the ionization chamber. One TLD was not exposed to radiation; it was kept behind the control panel to measure background radiation and light.

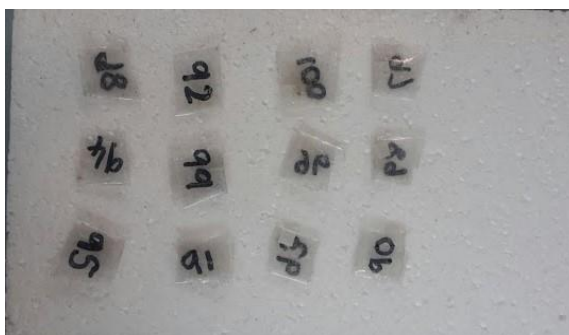


**Figure 3.3: Encapsulated TLDs placed on a polythene foam pad for calibration (Images acquired by the researcher for this research purposes)**

All TLDs were read in the Medical Physics Department at the research site using the REXON UL-320 TLD reader (Figure 3.8). The calibration factor for each TLD was mathematically calculated

and pre-programmed into the TLD reader to ensure that the correct calibration factor was used for each TLD every time. After reading, the TLDs were annealed using a PTW Freiburg annealing oven (Refer to 2.4.3.2.). Of the twelve TLDs that were calibrated for use for this research study, two were found to be defective and were thus excluded. This left ten TLDs that were available for use for this research study.

### **3.5.2. Air-kerma Area Product meter**

The KAP meters used for this study was fixed to the biplane angiography unit. These KAP meters display the readings in the units of  $\mu\text{Gy}\cdot\text{m}^2$  which were converted to  $\text{Gy}\cdot\text{cm}^2$  for this research study. The total KAP readings were displayed at the end of each procedure. The maximum entrance skin dose was also displayed in some cases (15 out of 34 cases). Annual calibrations are performed on the KAP meter in accordance with the ICRU (2005) and IAEA (2007) recommendations and South African Department of Health (2012) regulations.

### **3.6. Dose measurement methods**

Radiation dose measurements were performed during both the actual coil embolization studies and the phantom-based simulation studies.

#### **3.6.1. Actual coil embolization study**

Radiation dose measurements were performed on participants that underwent intracranial aneurysm coil embolization procedures. The Seldinger technique was used for the catheter insertion. During the embolization procedures, the intracranial artery of interest was selected in each patient and angiographic images were acquired in postero-anterior and lateral projections. These views were acquired using low magnifications (usually 32cm). A three dimensional rotational angiogram with 133 frames over 200 degrees rotation was performed when necessary to view the aneurysm in three dimensions. Following these initial angiogram images, the view that best demonstrated the aneurysm (here after referred to as 'the working view') was identified and the magnified images (16 cm or 11 cm) in that particular view were performed. A roadmap in the working view projection would then be used for micro-catheterization and coil deployment in the aneurysm.

To measure the radiation dose during this part of the study, two TLDs were placed on the participants. On average, three intracranial coil embolization procedures were performed per day. The TLDs were taped onto the participant's anterior neck in the midline, two fingers (about

4cm) above the supra-sternal notch (Figure 3.4). The TLD placement was done either by the researcher or by the research assistant. The TLDs were placed on the participants before the commencement of the procedure to ensure that the total radiation dose during the embolization procedure was measured. After each procedure, the TLDs were removed and stored in a light-proof container, away from the radiation area until they were read. All TLD readings were performed within 24 hours after the radiation exposure.

In addition, the total KAP, from both plane A and plane B KAP meters, was documented and used to determine the skin dose. The angiography unit also displayed maximum entrance skin dose for some of the procedures. Jaco and Miller (2010) suggest that the maximum entrance skin dose is the ideal dose metric for estimating the skin dose and deterministic risk to patients. Literature suggests that there is positive relationship between KAP and maximum entrance skin dose for neuro-interventional procedures (Theodorakou & Horrocks, 2003; D'Ercole et al., 2007; IAEA, 2010). The available information on the maximum entrance skin dose was used to determine whether there was positive relationship between KAP and maximum entrance skin dose during the current study. All the collected data were documented on a data collection sheet (Appendix B1).



**Figure 3.4: Simulated TLD positioning on the anterior neck of patients  
(Images acquired by the researcher for this research purposes)**

### 3.6.2. Phantom-based simulation studies

After all data were collected during actual coil embolization studies, phantom-based simulation studies were carried out. The purpose of the phantom-based studies was to evaluate the difference between the radiation dose measured at the anterior neck over the thyroid region and the dose measured directly at the anatomical area of the thyroid gland. This measurement was necessary, as it was not possible to perform direct thyroid measurements on a human being.

A male upper body Alderson's RANDO phantom was used (Figure 3.5). A RANDO phantom consists of natural human skeleton and material that is radiologically equivalent to human soft tissue. This phantom has transverse slices with removable parts. This enabled the researcher to measure the radiation dose to the thyroid gland, as the measuring device could be placed directly at the anatomical thyroid gland location of the phantom.

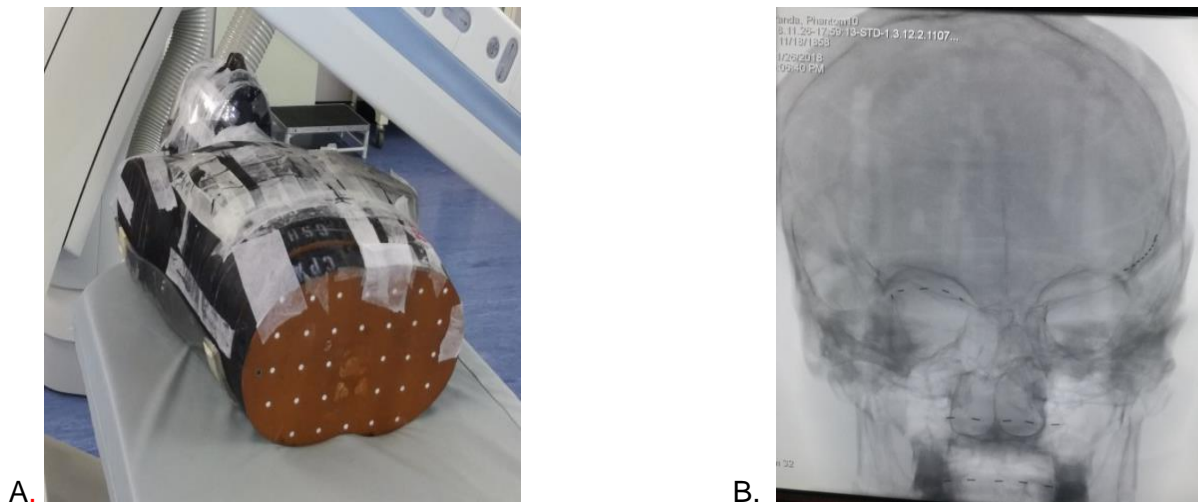


**Figure 3.5: A. RANDO phantom; and B. Postero-anterior radiographic skull view of the RANDO phantom (Images acquired by the researcher for this research purposes)**

Intracranial aneurysm coiling procedures were simulated on the phantom using the fluoroscopic angles, fluoroscopy times and angiography acquisition factors similar to those used during the actual coil embolization procedures. The following scenarios were simulated:

- the procedure that had the shortest fluoroscopy time during the embolization procedures;
- the procedure that had the medium fluoroscopy time during the embolization procedures;
- and
- the procedure that had the longest fluoroscopy time during the embolization procedures.

The angiographic examinations that met the above criteria were identified from the actual coil embolization data collection sheet. The Picture Archiving and Communication System (PACS) was used to extract the parameters, e.g. number of exposures, the C-arm angulation and magnification as well as angiography imaging parameters that were used for each individual coil embolization study and these were replicated. The distance between the image intensifier and the patient was not measured and documented and therefore could not be replicated during the simulations. The image intensifier was positioned as close to the phantom as possible for all simulations. The collimation during the patient studies was not constant and thus it was not replicated during the phantom based simulation studies. However, the collimation was constant for all simulation studies. Table 3.1 shows the imaging data for each simulated scenario.

**Table 3.1: Imaging data for the simulated scenarios**

	Scenario 1 (shortest fluoroscopy time)	Scenario 2 (medium fluoroscopy time)	Scenario 3 (longest fluoroscopy time)
<b>Fluoroscopy time (minutes)</b>	4.9	22	41.1
<b>KAP (Gy.cm<sup>2</sup>)</b>	36.6	33	77.8
<b>No. of exposures/ runs</b>	12	10	22
<b>No. of image frames</b>	368	372	534
<b>Working view</b>	LA0 90°	LAO 130°cranial 30°	RA0 30° caudal 45°

To ensure reliability and validity of results, the simulation of each scenario was repeated three times, making sure that all factors remained the same. For each simulation, four TLDs were placed on the phantom to measure the radiation dose. Two TLDs were placed on the thyroid gland hole while the other two TLDs were placed on the anterior neck of the phantom, over the thyroid region (Figure 3.6). There were ten TLDs available for this research study and therefore only two phantom based simulation studies could be performed at a time. The thyroid hole extends over slices nine and ten of the RANDO phantom. For this study, the thyroid hole on the cranial end of slice 10 was used for TLD placement as this corresponded well with the TLD



positioning on the participants during the actual aneurysm coil embolization. Acun et al. (2007) also placed the TLDs on the tenth slice of the RANDO phantom for the thyroid gland dose measurements during their research study. After the exposure, the TLDs were sent for reading and the information was documented on a separate data collection sheet (Appendix B2).

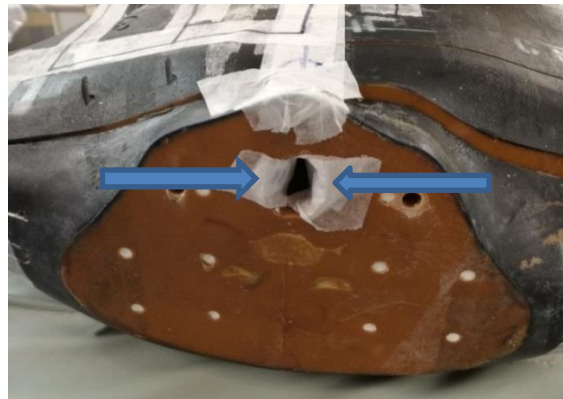


**Figure 3.6: TLD positioning on the top end of slice 10 of the RANDO phantom (blue arrows) corresponding with the anatomical location of the thyroid gland (Images acquired by the researcher for this research purposes)**

### **3.7. Equipment**

#### **3.7.1. Intracranial aneurysm embolization equipment**

The intracranial aneurysm coil embolization procedures and the phantom studies were performed using a Siemens Artis Zee biplane angiographic unit manufactured in Germany in 2014. The unit has 30x40 cm flat panel detectors on both C-arms and an under-couch x-ray tube on the C-arm for plane “A”. The C-arm for Plane “A” was floor-mounted and was used in the postero-anterior position while the C-arm for plane “B” was ceiling-mounted and operated in the lateral position. The half value layer (HVL) of this unit is 2.7 mm aluminium (Al) at 75 kV. Both x-ray tubes are fitted with permanent KAP meters for radiation dose measurements. Routine quality assurance and servicing was performed on the angiography unit.

During examinations, the kV and mA are automatically adjusted using automatic exposure control (AEC) technology, in accordance with the patient’s body habitus as well as the x-ray tube angulations. The low dose neuro-radiology program with Combined Applications to Reduce

Exposure (CARE) was used with the fluoroscopy frame rate of 10 pulses per second and the angiographic acquisition frame rate of 4 frames per second for all procedures.

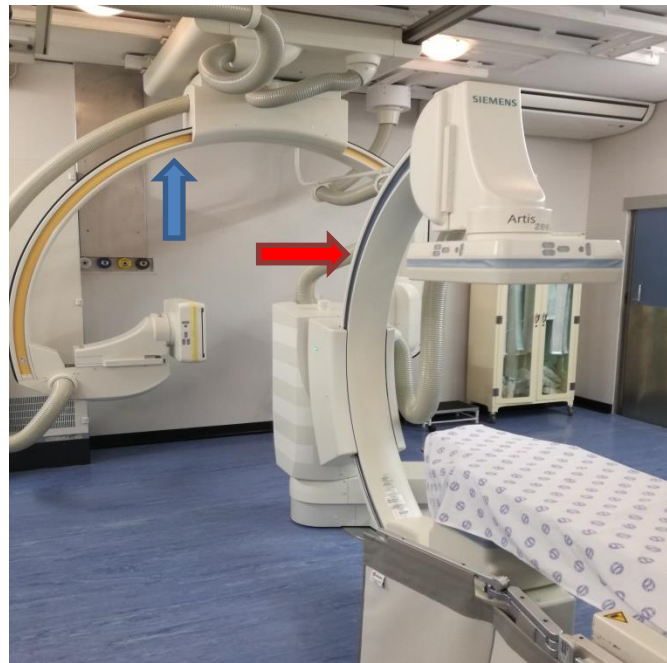


**Figure 3.7: Siemens Artis Zee biplane angiography unit used for the aneurysm coil embolization procedures at the research site. Red arrow indicates plane “A” C-arm, blue arrow indicates plane “B” C-arm. (Images acquired by the researcher for this research purposes)**

### 3.7.2. TLD reader

A Rexion UL-320 TLD reader was used for the study. This TLD reader was connected to a computer and operated on a Windows program. TLD reading is performed in a nitrogen atmosphere to avoid oxidation that could affect the readings, therefore the TLD reader was also connected to a nitrogen gas cylinder.

The Rexion TLD reader was compatible to a wide range of TLD material chips, rods and discs. To improve accuracy, this TLD reader was calibrated for the LiF TLDs before it was used for the current study. The cycle time varies between 0 and 3 minutes. The heating temperature cycle was user controlled. The maximum temperature used at the research site for TLD reading is 280 degrees Celsius. The Rexion TLD reader also had annealing capabilities, but the TLDs were annealed using the annealing oven during the present study.



**Figure 3.8: A REXON UL –320 TLD reader used for reading TLDs at the research site (Images acquired by the researcher for this research purposes)**

### **3.7.3. TLD annealing oven**

The TLDs were annealed using a PTW – Freiburg TLDO automatic TLD oven, manufactured in Germany. After reading, the TLDs were put on the annealing tray according to their place numbers (to avoid TLD mix-up and thus reading TLDs using incorrect calibration factors) and placed in the annealing oven to remove all residual traps before re-use. The annealing procedure used was 1 hour at a temperature of 400°C followed by 2 hours at 100°C. The TLDs were subsequently left in the oven overnight for cooling.

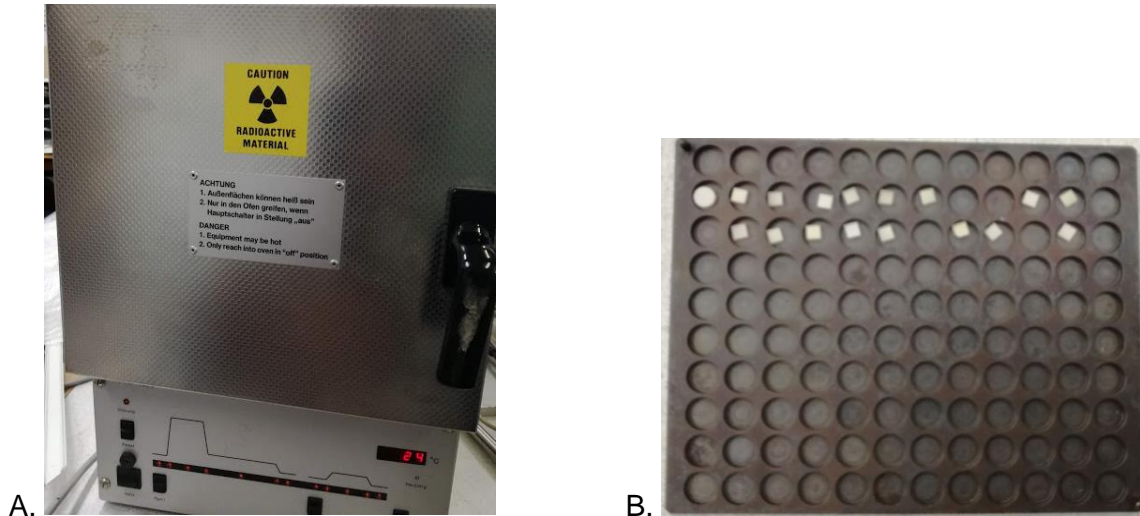


**Figure 3.9: A. PTW – Freiburg TLDO annealing oven used for TLD annealing at the research site; B: TLD placement on the annealing tray (Images acquired by the researcher for this research purposes)**

### 3.8. Dose calculations

#### 3.8.1. Thyroid absorbed dose

The thyroid absorbed dose was determined by calculating the difference between the radiation dose measured on the anterior neck and the radiation dose measured directly on the thyroid gland during the phantom-based simulation study. The difference between the two measurements was then factored into the TLD readings obtained from the anterior neck of each patient to obtain the thyroid absorbed dose value.

#### 3.8.2. Thyroid equivalent dose

The equivalent dose was calculated by multiplying the absorbed dose by the radiation weighting factor for x-rays using Equation 1.

#### 3.8.3. Diagnostic Reference Levels

The total KAP from both plane “A” and plane “B” KAP meters, the fluoroscopy time and the number of frames were used to determine the DRLs. The KAP meters attached to the angiography unit used in the current study displayed the readings in the units of  $\mu\text{Gy}\cdot\text{m}^2$  which were converted to  $\text{Gy}\cdot\text{cm}^2$  by dividing the value by 100. The 3<sup>rd</sup> quartile of the KAP value, the

fluoroscopy time and the number of image frames were set as the diagnostic reference level for intracranial aneurysm coil embolization at the research site.

#### **3.8.4. Monte Carlo calculations**

The Monte Carlo program PCXMC 2.0 by STUK, 2008, Finland was used to calculate the radiation doses to the thyroid gland and the skin. The KAP (in mGy.cm<sup>2</sup>), kV and the x-ray beam angulation documented during the patient study were entered into the PCXMC software for dose calculations. The focal spot to skin distance (FSD) ranged between 65 cm and 80 cm during actual coil embolization procedures. This was however not documented for all patients during data collection. A decision to use a standard FSD of 65cm for all Monte Carlo calculations was taken. The x-ray field size and patients' weight and height were not measured during data collection and therefore the default values on PCXMC were used for all calculations. The default patient weight was 73.2 kg and patient height was 1.78 metres. Additional parameters used for calculations are listed in table 3.2. The dose values obtained from the Monte Carlo calculations were compared to the measured doses to determine whether there was correlation between the measured and calculated doses.

**Table 3.2: Parameters used for dose calculations in the PCXMC program**

Parameter	Value
X Ref	<b>0</b>
Y Ref	<b>0</b>
Z Ref	<b>85</b>
X-ray field size	<b>20 x 20 cm<sup>2</sup></b>
Number of photons	<b>20 000</b>
Anode angle	<b>14°</b>
Filtration	<b>2.7 mm Al + 0.1 mm Cu</b>

### **3.9. Data collection and analysis**

During the aneurysm coil embolization procedures on patients, the collected data included the following: the aneurysm location, the fluoroscopy time, DAP reading, TLD identification number, TLD readings and technical factors, i.e., kV, “the working view” and number of image frames. The patients’ age and gender were also documented (Appendix B1). Aneurysms were grouped according to their locations and each location was assigned a number for statistical analysis purposes.

The data collected during the phantom based simulation studies included fluoroscopy time, KAP reading, TLD reading on the thyroid gland and the TLD reading on the anterior neck. TLD readings were analysed for the difference between the radiation dose measured on the anterior neck and the radiation dose measured on the thyroid gland. This information was then used to determine the radiation dose to the participants’ thyroid glands during intracranial aneurysm coil embolization.

### **3.10. Ethical considerations**

The Declaration of Helsinki requires all medical research involving human participants to be approved by a research ethics committee (World Medical Association, WMA, 2013). Ethics approval for this research study was granted by the Cape Peninsula University of Technology’s Faculty of Health and Wellness Sciences Research Ethics Committee (CPUT/HW-REC 2017), as well as the University of Cape Town’s Faculty of Health Sciences Human Research Ethics Committee (HREC REF: 471/2017). Permission to conduct the study was also granted by the Hospital’s Research Committee (Certificates attached as Appendices C1 - C3). The heads of the Radiology and Neurosurgery departments also granted verbal permission for the study to be conducted.

The principles of the Declaration of Helsinki were upheld throughout the duration of the study. One of these principles states that voluntary informed consent should be obtained from participants and those participants who have low levels of consciousness and those who are considered as vulnerable participants should be excluded, unless the research can be performed on these participants only (WMA, 2013). In line with these principles, patients who had low levels of consciousness and those who were regarded as vulnerable participants, for example children and psychiatric patients were excluded from the study. Informed consent was sought from all patients who were deemed eligible to participate in the study. Patients who were

booked for coil embolization procedures were approached in the neurosurgical ward to assess their eligibility for participation in the research study. Those who were found to be eligible for participation were recruited using the information sheet and a verbal explanation was provided by the researcher or research assistant. Participants gave informed consent by signing or putting a thumb print on the informed consent form (Appendix D). Participation in the study was completely voluntary, i.e. the research participants were not coerced in any way to participate in the study and they were informed of their right to refuse to participate in the study.

The principles of the Declaration of Helsinki further state that the research participants should not be subjected to risk or harm as part of the study and if risk cannot be avoided, it should be kept to a minimum (WMA, 2013). The Medical Research Council (MRC) (2002) set guidelines for research involving the use of ionizing radiation. These guidelines state that radiation related research studies should:

- Avoid inclusion of research participants that are younger than 40 years of age due to the increased risk of detrimental effects of ionizing radiation in younger people and children.
- Include a detailed statement of the source and nature of radiation and explanation of estimated radiation risks to the participants.
- Calculation of the absorbed dose should be done.

These MRC guidelines did not apply to this study as the research participants were not subjected to any additional radiation for the purposes of this research study. The dose measurements were performed during the normal routine intracranial aneurysm embolization examinations for which patients had been referred.

There were no risks, harm or benefits to the patients that participated in this study. There were also no adverse events to the patients as a result of the research study. The patients' anonymity was ensured by saving the research data without the patients' identity – each participant was assigned a study number. Furthermore, the research data was kept confidential by securing all hard copies of signed consent forms and data collection sheets in a locked cupboard and all electronic copies were password-protected.

The daily workflow and management of the Vascular Radiology Department at the research site were not interrupted as a result of this research study. The researcher also did not use any consumables from the research site.

### **3.11. Conclusion**

The aim of this study was to determine the average radiation dose received by patients during intracranial aneurysm coil embolization. The methodology that was employed during the current study, to achieve the aim of the study, was discussed in detail in this chapter. The next chapter, Chapter 4, will explain the results of the current research study. Chapter 5 thereafter will discuss and compare our results to those of previously published local and international studies to assess whether dose levels at the research site are comparable to doses from the published studies.



## **CHAPTER 4: RESULTS**

### **4.1. Introduction**

This chapter will provide a brief overview of the data analysis conducted, followed by the findings of the research study. The aim of this study was to determine the average radiation dose to patients' thyroid glands and skin during intracranial aneurysm coil embolization procedures. The radiation dose to the anterior neck over the thyroid gland region of participants was measured using TLDs. In addition, phantom-based simulation studies were performed to evaluate the difference between the radiation dose measured on the anterior neck over the thyroid gland region and the dose measured at the anatomical location of the thyroid gland (Figure 3.6). It was necessary to perform these dose measurements on the phantom as it is not possible to perform direct thyroid gland measurements on human beings. Imaging was performed using a biplane angiography unit with an under-couch x-ray tube for the C-arm for plane "A" and therefore postero-anterior views were acquired. This resulted in the thyroid doses being more than the anterior neck doses due to the attenuation of the beam before reaching the anterior neck. The difference between the thyroid gland measurements and the anterior neck measurements was added to the dose measurements obtained on the anterior neck of participants to determine the thyroid absorbed dose on patients. The radiation doses to the thyroid glands and skin were also calculated using the Monte Carlo method, and comparison was made between the measured doses and the calculated doses.

The KAP meters attached to the angiography unit were used for patients' skin dose estimation. The maximum entrance skin dose was also displayed by the angiography unit for 15 out of 34 procedures. When numerous different x-ray tube angulations were employed during the procedure, it was difficult for the angiography unit to determine the area of highest exposure. This could explain why maximum entrance skin dose was not displayed for all the procedures included in the current research study. 'Maximum entrance skin dose' referred to the radiation dose to the most irradiated area of the skin during fluoroscopy guided procedures. Maximum entrance skin dose was the preferred dose metric to estimate the deterministic risk to patients (Jaco & Miller, 2010). The available information on the maximum entrance skin dose was used to determine the correlation between KAP and maximum entrance skin dose.

DRLs for intracranial aneurysm coil embolization procedures were also established during the current study. According to the IAEA (2016), DRLs should be set at hospital level, regional level

and at national level for all common radiological procedures, as well as for procedures that result in high radiation doses. As mentioned in section 1.4 there is paucity in DRLs for neuro-embolization procedures in South Africa. The recommended dose metrics for setting DRLs for fluoroscopically guided procedures are KAP, fluoroscopy time, cumulative dose and number of image frames; and the 75<sup>th</sup> percentile of these dose metrics is used (ICRP, 2017). The 75<sup>th</sup> percentile of KAP, fluoroscopy time and number of image frames were used for establishing DRLs during the current study.

In this chapter, the measured thyroid absorbed doses, the KAP values, the Monte Carlo calculated thyroid gland and skin doses as well as DRLs for intracranial aneurysm coil embolization, are reported.

## **4.2. Data analysis**

IBM Statistical Package for Social Sciences (SPSS®) 2018 and Windows Microsoft® Excel 2010 were used for data analysis. Excel was used to determine the percentage difference between the radiation dose measured on the anterior neck and the dose measured directly on the thyroid gland during the phantom based studies. The characteristics of the research participants and the participants' age distribution, as well as aneurysm location distribution, were also determined using Excel. SPSS was used for correlation and relationship statistics, as well as to determine the 75<sup>th</sup> percentile of radiation doses.

### **4.2.1. Descriptive statistics**

The sample population included 34 research participants: eleven males (32%) and 23 females (68%). Thirty of the 34 participants had aneurysm coil embolization procedures. Four participants had no coil embolization. These patients had diagnostic cerebral angiography only. Of the four participants that had diagnostic cerebral angiography, no aneurysms could be identified in three cases and one participant had an aneurysm that was not suitable for coil embolization. The age of participants ranged from 18 to 70 years with the majority of participants (16 out of 34) between the ages of 46 and 55 years. The age distribution of the research participants is shown in Figure 4.1.

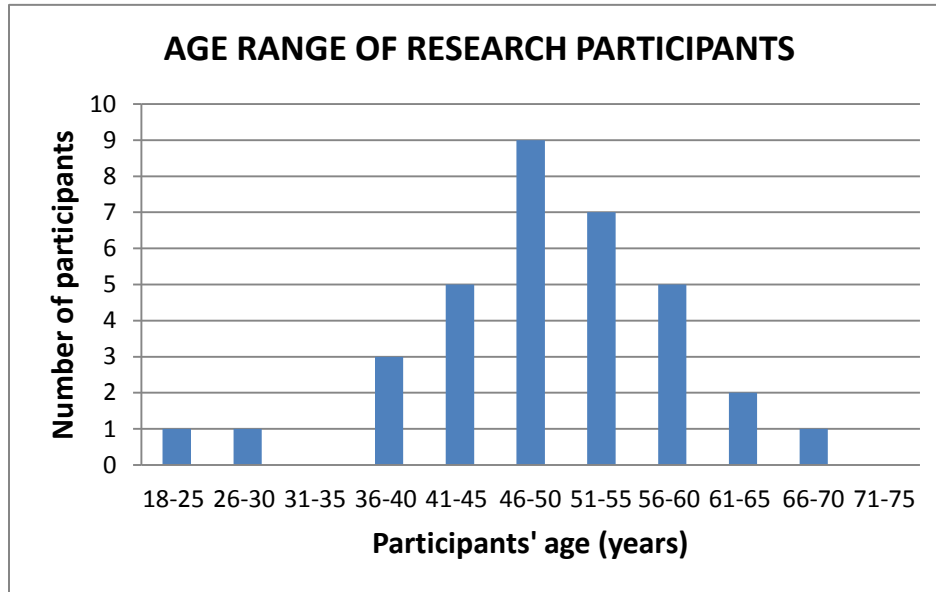


**Figure 4.1: Age distribution of research participants**

#### **4.2.2. Inferential statistics**

Inferential statistics were performed to determine whether the anatomical location of the aneurysm had an effect on the radiation dose during intracranial aneurysm coil embolization. The aneurysm anatomical locations were grouped into 10 categories. Some of the aneurysm location categories had a sample size of less than five. Because of the afore-mentioned reasons, Kruskal Wallis was the non-parametric statistical test of choice as it can be used to test for differences between two or more groups of an independent variable. This statistical test can also be used when the sample in each group has fewer than five participants, with each group consisting of different participants (Burns & Grove, 2005:525).

Correlation statistics were also performed during the current study. Correlation coefficients are used to determine whether there is a relationship, as well as the nature of a relationship, between two variables (Peat & Barton, 2005: 157). In the present study, Spearman's correlation test was used to determine whether there was correlation between the KAP values and the number of image frames, as well as between the KAP values and the maximum entrance skin dose. Spearman's correlation is the correlation coefficient of choice for ordinal and categorical data (Peat & Barton, 2005:157) and, as the research data was ordinal in nature, Spearman's correlation test was chosen for the current study. In addition, scatter graphs were plotted to

determine the nature of the relationship between the KAP and the number of image frames, and between the KAP and the maximum entrance skin dose.

### **4.3. Phantom-based simulation studies (PBSS)**

The phantom-based simulation studies set out to measure the dose on the anterior neck over the thyroid region as well as at the anatomical location of the thyroid gland to determine the difference between the dose measured on the anterior neck and the dose measured directly on the thyroid gland. During the PBSS, TLDs were placed on the anterior neck as well as in the thyroid gland hole of the phantom for each simulation. Three different intracranial aneurysm coil embolization scenarios were simulated. These scenarios were as follows:

**Scenario 1:** The procedure that had the shortest fluoroscopy time which was 4.9 minutes during the actual coil embolization studies.

**Scenario 2:** The procedure that had a medium fluoroscopy time (22 minutes) during the actual coil embolization studies.

**Scenario 3:** The procedure that had the highest fluoroscopy time (41.1 minutes) during the actual coil embolization studies.

Each scenario was intended to be repeated three times to ensure reliability of results. However, for scenario 2, the TLDs gave inconsistent readings, i.e. the doses were not in the same range for the first three simulations. The anterior neck doses were 14 mGy, 8 mGy and 14.5 mGy for simulation 1, simulation 2 and simulation 3 respectively. Because of these inconsistent readings, another three simulations were performed for scenario 2 to ensure reliability of measurements. This resulted in a total of 12 simulations. The results of the PBSS are shown in Table 4.1. Four of the six anterior neck TLD readings for scenario 2 were in the same range (6.5 to 8 mGy), while the other two readings were higher (14 and 14.5 mGy respectively). For scenario 1, one of the three TLD readings for both the anterior neck and the thyroid doses was higher than the rest, while one of the three readings for the anterior neck was higher than the rest for scenario 3. These high readings (highlighted in yellow in Table 4.1) were considered inaccurate, either owing to experimental errors or to errors in TLD readings, so were excluded from the final calculations. The decision to exclude the high readings was based on a study by Rybicki et al. (2002) in which a similar finding was reported.

**Table 4.1: Measurements obtained from PBSS**

STUDY	FLUORO TIME (min.)	KAP (Gy.cm <sup>2</sup> )	ANTERIOR NECK TLD READING (mGy)			THYROID TLD READING (mGy)			*DIFFERENCE	% DIFF	
			TLD 1	TLD 2	MEAN	TLD 1	TLD 2	MEAN			
SCENARIO 1	SIM 1	3.5	25.5	3.0	2.0	2.5	6.0	4.0	5.0	2.5	100
	SIM 2	3.3	22.4	3.0	2.0	2.5	4.0	4.0	4.0	1.5	60
	SIM 3	3.5	23.8	5.0	4.0	4.5	13.0	8.0	10.5	6.0	133
SCENARIO 2	SIM 1	22.0	37.7	16.0	12.0	14.0	20.0	15.0	17.5	3.5	25
	SIM 2	21.7	29.5	9.0	7.0	8.0	11.0	10.0	10.5	2.5	31
	SIM 3	22.3	33.4	17.0	12.0	14.5	20.0	19.0	19.5	5.0	35
	SIM 4	22.1	30.0	8.0	7.0	7.5	12.0	11.0	11.5	4.0	53
	SIM 5	21.9	28.7	8.0	6.0	7.0	13.0	10.0	11.5	4.5	64
	SIM 6	22.5	31.9	7.0	6.0	6.5	12.0	11.0	11.5	5.0	77
SCENARIO 3	SIM 1	40.5	55.5	8.0	7.0	7.5	12.0	11.0	11.5	4.0	53
	SIM 2	40.5	58.5	8.0	8.0	8.0	12.0	12.0	12.0	4.0	50
	SIM 3	40.4	60.7	13.0	8.0	10.5	14.0	12.0	13.0	2.5	24

SIM = simulation;

\*DIFFERENCE = Difference between anterior neck and thyroid TLD readings in mGy;

\*% DIFF = Percentage difference between anterior neck and thyroid TLD readings

$$\text{Percentage difference} = \frac{\text{Thyroid TLD reading} - \text{anterior neck TLD reading}}{\text{Anterior neck TLD reading}} \times 100 \quad (\text{Equation 2})$$

For the remaining eight phantom simulations, the percentage difference between anterior neck radiation dose and the thyroid gland radiation dose was found to range between 31% and 100% with an average of 61%. In addition to calculating the overall average percentage difference for all eight simulations, the average percentage difference was also calculated for each scenario. The average percentage difference was 80% for scenario 1, 56% for scenario 2 and 52% for scenario 3. The average percentage difference for each scenario was then applied to the anterior neck dose values obtained from the procedures where the corresponding working view was employed during the actual coil embolization study. This meant that for scenario 1, for example, the working view was LAO 90° and the average percentage difference was 80% and therefore 80% was added to all cases where the LAO 90° working view was employed during the actual coil embolization study. The 61% overall average percentage difference was used in all cases where there was no corresponding working view during the phantom-based simulation studies. For all 8 simulations, the thyroid doses were higher than the neck doses due to the fact there was more attenuation of the x-ray beam before reaching the anterior neck as the images were acquired in postero-anterior projection. Therefore, the percentage difference was added to the anterior neck readings. Figure 4.2 shows the difference between the anterior neck dose and the thyroid dose.

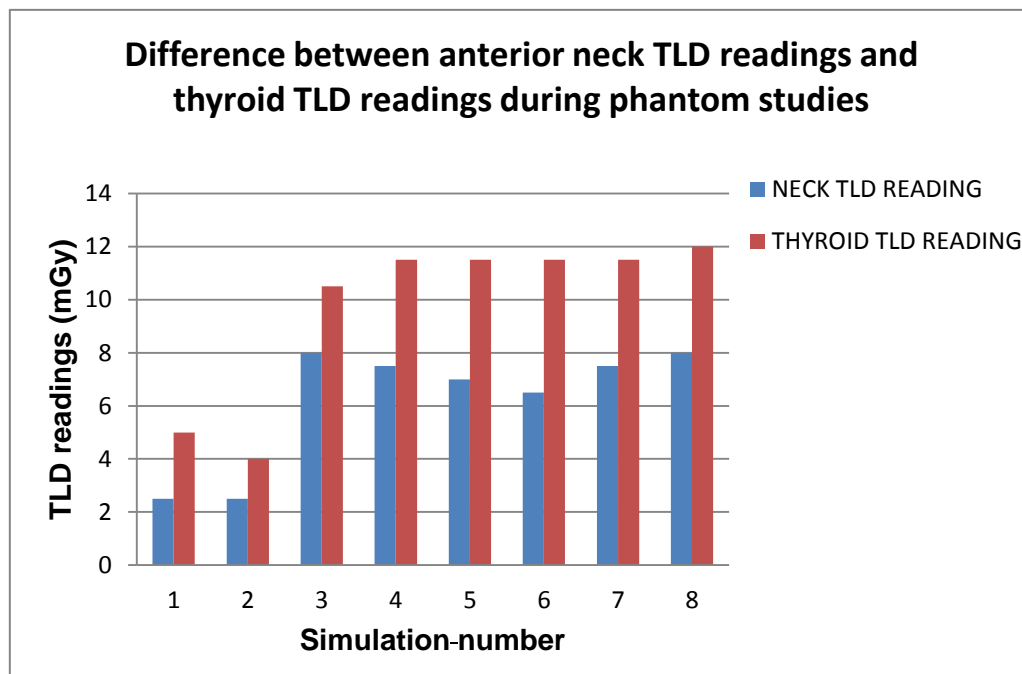


Figure 4.2: Results of the phantom-based simulation studies

#### **4.4. Radiation dose to the thyroid gland**

Thyroid absorbed doses and thyroid equivalent doses to the patients were determined during the current study. The absorbed dose is the amount of ionizing radiation deposited on a tissue or organ. The absorbed dose does not take the type of radiation or the biological effects of different types of radiation into account. An equivalent dose, on the other hand, is used to determine the radiation dose, taking into account the different biological effects to tissues due to different types of radiation (Muhammad et al., 2017).

##### **4.4.1 Thyroid absorbed doses**

Radiation doses to the participants' anterior neck were measured using TLDs during the actual coil embolization studies. The absorbed doses to the thyroid glands of participants were then calculated by adding 61% (which was found to be the difference between the anterior neck dose and the thyroid dose) to the value obtained from the anterior neck during actual coil embolization studies. Table 4.2 lists the anterior neck doses and thyroid absorbed doses to the participants.

**Table 4.2: Anterior neck doses obtained from TLD measurements and calculated thyroid absorbed doses to participants**

STUDY NUMBER	ANTERIOR NECK RADIATION DOSE (mGy)	THYROID ABSORBED DOSE (mGy)
1	3.50	*6.30
2	7.00	11.28
3	10.00	16.11
4	7.00	11.28
5	2.00	3.22
6	9.00	*14.50
7	3.50	5.60
8	9.50	15.31
9	6.00	*9.67
10	4.50	7.24
11	5.00	8.06
12	2.00	*3.22
13	7.50	12.10
14	6.50	10.47
15	11.00	#17.71
16	6.50	*10.17
17	7.00	12.60
18	2.50	4.03
19	6.50	10.47
20	8.50	13.20
21	8.00	12.90
22	5.00	*8.06
23	9.00	14.50
24	10.00	18.00
25	3.50	5.64
26	7.50	*12.10
27	13.00	20.95
28	5.00	*8.06
29	9.00	*16.20
30	11.00	17.63
31	11.50	20.70
32	4.00	6.45
33	10.50	*18.90
34	13.00	20.95

\*Represents calculated thyroid doses which include the 80% difference between anterior neck and anatomical thyroid gland dose; # represents calculated doses which include 56% difference; the rest were calculated using 61% difference.



The mean and the median values and the standard deviation of all 34 thyroid absorbed doses listed in Table 4.2 were calculated using Microsoft® Excel 2010. The minimum, mean, median and maximum thyroid absorbed doses to participants are listed in Table 4.3.

**Table 4.3: Thyroid absorbed doses to the participants**

PARAMETER	DOSE (mGy)
<b>Minimum thyroid dose</b>	3.22
<b>Median thyroid dose</b>	10.47
<b>Mean (Standard deviation)</b>	11.25 (5.49)
<b>Maximum thyroid dose</b>	20.95

#### **4.4.2. Thyroid equivalent doses**

The equivalent dose was calculated by multiplying the absorbed dose by the radiation weighting factor for x-rays as in Equation 1

Because the radiation weighting factor for x-rays is equal to 1, the equivalent dose has the same numerical value as the absorbed dose. However, the equivalent dose is measured in units of Sievert (Sv) to express the biological response to radiation. Therefore, the thyroid equivalent doses for the current study were found to be between 3.22 mSv and 20.95 mSv and the mean thyroid equivalent dose was 11.25 mSv.

#### **4.4.3. Monte Carlo calculated thyroid doses**

In addition to TLD measurements, thyroid doses were also calculated using PCXMC software. The calculated thyroid doses ranged between 4.50 and 40.47 mGy with a mean of 16.11 mGy. Figure 4.3 shows no correlation between measured and calculated thyroid doses. There was also no correlation between KAP and PCXMC calculated thyroid doses.

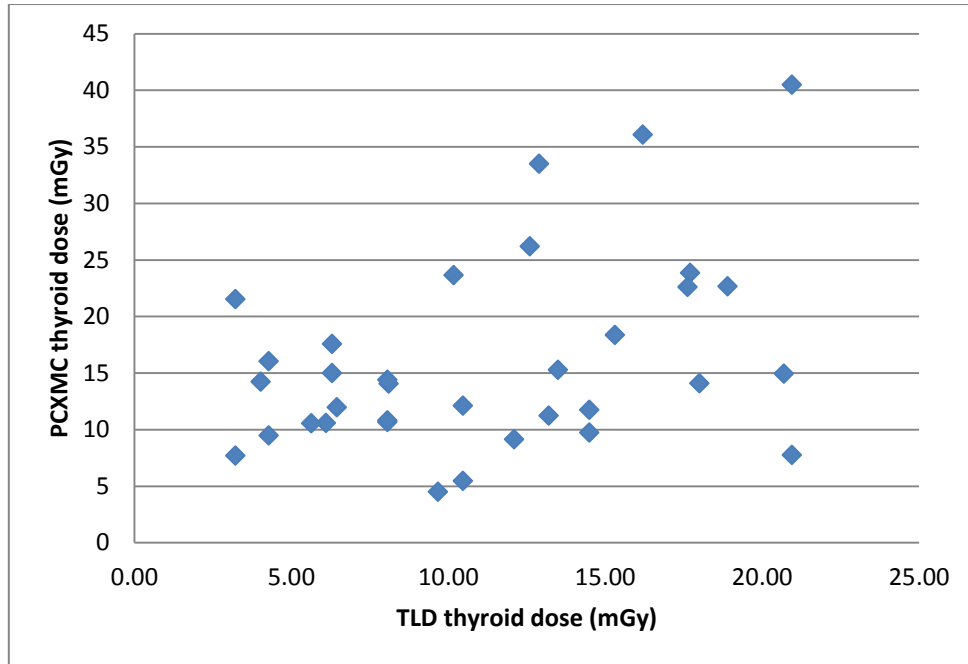


**Figure 4.3: Comparison between TLD measured and PCXMC calculated thyroid doses**

#### **4.5. Radiation dose to the skin**

The study included 34 participants: 30 had aneurysm coil embolization and 4 had diagnostic cerebral angiography. During the current study, the radiation dose to the participants' skin was determined using a KAP meter attached to the angiography unit and calculated using PCXMC software. The next section describes the results obtained from the skin dose measurements.

##### **4.5.1. Radiation dose to the skin as determined by the KAP meter**

The KAP values were displayed at the end of each procedure. The angiography unit also displayed the maximum entrance skin dose at the end of the procedure. The entrance skin dose was, however, only displayed for 15 out of the 34 procedures included in the current study. The maximum entrance skin dose ranged between 186 and 697 mGy with the mean of 360 mGy. The KAP values obtained during the study for all procedures, including diagnostic only and coil embolization procedures, are listed in Table 4.4.

**Table 4.4: KAP values from the current study**

DAP (Gy.cm <sup>2</sup> )		
N	Valid	34
	Missing	0
Mean		56.2
Median		53.1
STDEV		19.9
Minimum		33.0
Maximum		125.7
Percentiles	25	40.2
	50	53.1
	75	68.1

The KAP values for all procedures, coil embolization procedures and diagnostic-only procedures are listed separately in Table 4.5. As shown in Table 4.5, there was no significant difference between the KAP values for diagnostic-only procedures and aneurysm coil embolization procedures. However, these results should be interpreted with caution due to the difference in the sample size in each group.

**Table 4.5: KAP values according to type of procedure**

Type of procedure	No. of cases	KAP (Gy.cm <sup>2</sup> )			
		Minimum	Median	Mean	Maximum
<b>All procedures</b>	34	33.0	53.0	56.1	125.7
<b>Coiling only</b>	30	33.0	52.1	56.3	125.7
<b>Diagnostic only</b>	4	38.1	57.3	55.1	67.9

#### 4.5.2. Monte Carlo calculated skin doses

In addition to using the KAP meter to determine skin doses, the skin dose was also calculated on PCXMC. The calculated doses were compared to the KAP values to determine whether there was correlation between the two dose values. Both the power fit and linear fit showed a strong positive correlation between the KAP measured skin dose and the calculated dose ( $R^2=0.933$ ). This means that KAP provided a similar result to the PCXMC in determining the skin dose. Figure 4.4 shows the power fit between KAP value and the PCXMC skin dose.

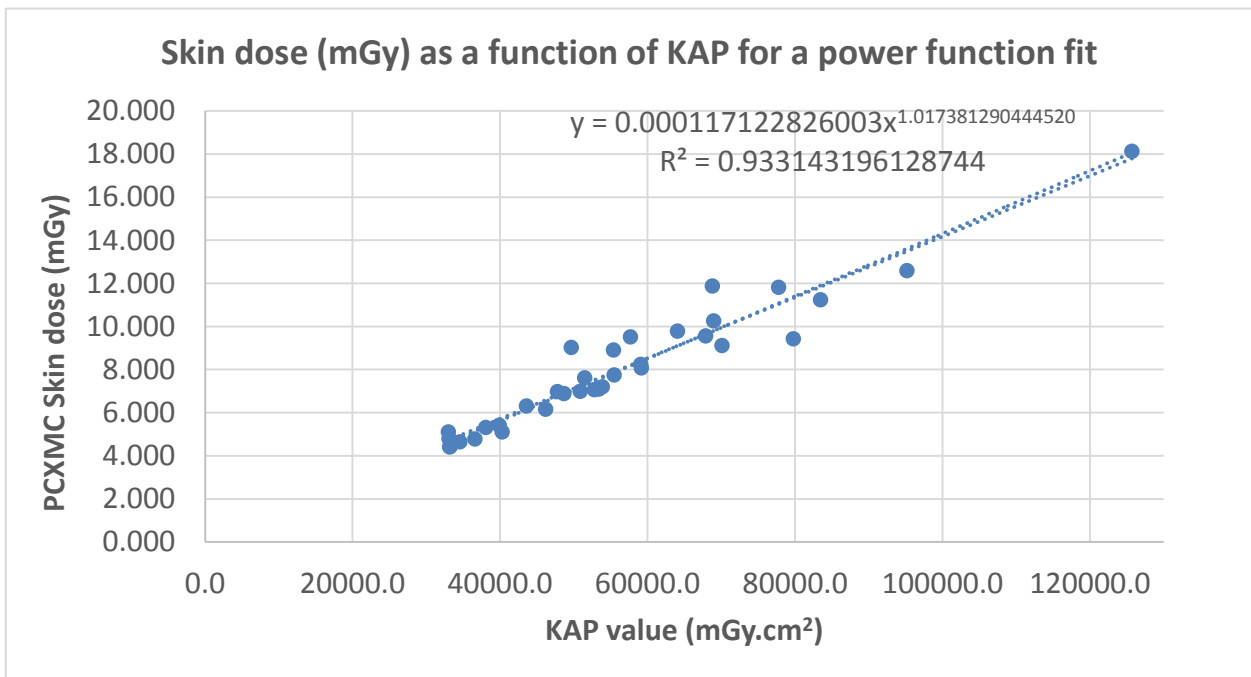
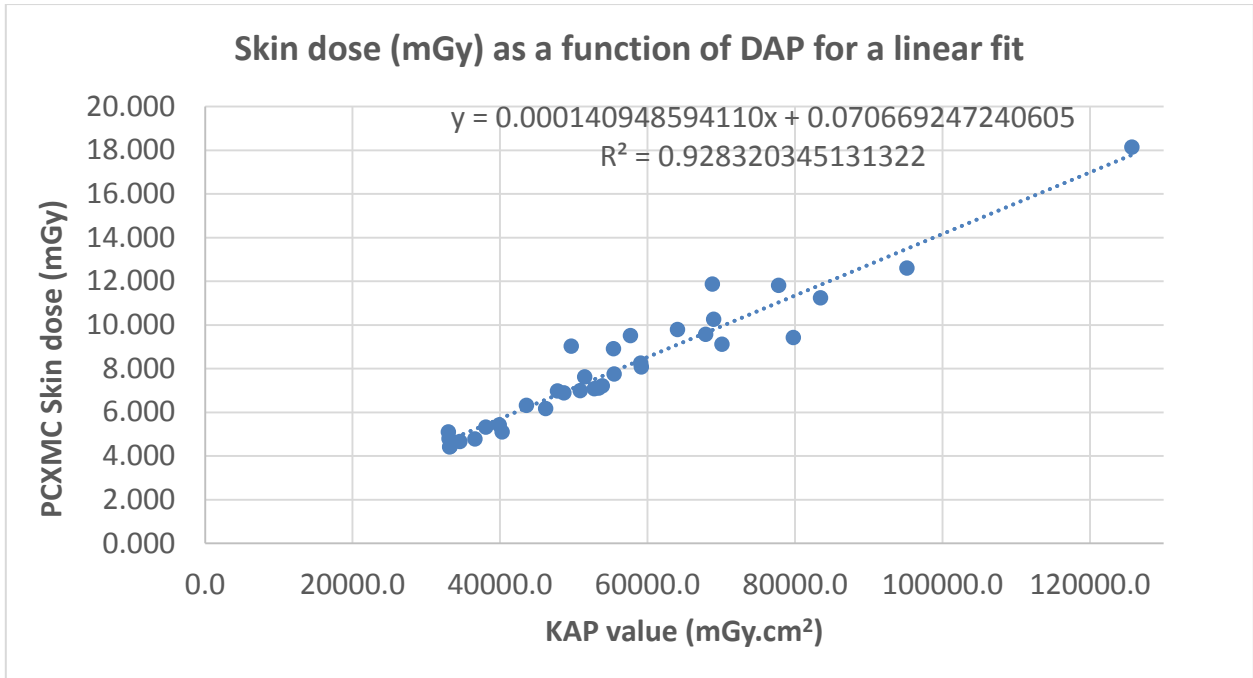


Figure 4.4: Power fit between measured and calculated skin dose

Figure 4.5 shows the linear fit between KAP value and PCXMC calculated skin dose.



**Figure 4.5: Linear fit between measured and calculated skin dose**

#### **4.6. Effect of aneurysm location on the radiation dose**

According to Acton et al. (2018), the aneurysm location has the most substantial effect on the patient radiation dose during intracranial aneurysm coiling. Aneurysms that are situated in difficult to reach areas may result in an increased radiation dose to patients, as prolonged fluoroscopy would be required to place the catheter successfully in the aneurysm. Complex aneurysms also warrant additional image acquisitions to define clearly the aneurysm and its neck, resulting in an increased radiation dose to patients (Acton et al., 2018).

During intracranial aneurysm coil embolization, use of steep angulations (more than 30 degrees angulation of the x-ray tube) which have been reported to lead to increased radiation doses to patients (NCRP, 2011), is sometimes warranted. The x-ray tube angulation is determined by the aneurysm location and the view that best shows the aneurysm is used for guiding the catheter and embolization coils into the aneurysm. This suggests that an aneurysm that requires the use of steep angulations during fluoroscopy and image acquisition would result in an increased radiation dose to the patient compared to an aneurysm that requires use of a straight x-ray tube.

One of the objectives of the current study was to establish whether anatomical location of the intracranial aneurysm affects the radiation dose to patients.

Thirty one of the 34 participants in the current study presented with intracranial aneurysms in different anatomical locations. Four of these participants presented with more than one aneurysm but only one aneurysm, the one that bled, was embolized in each participant. The majority of the aneurysms were located at the origin of the posterior communicating artery (PCom) followed by the anterior communicating artery (ACom) aneurysms (Figure 4.6).

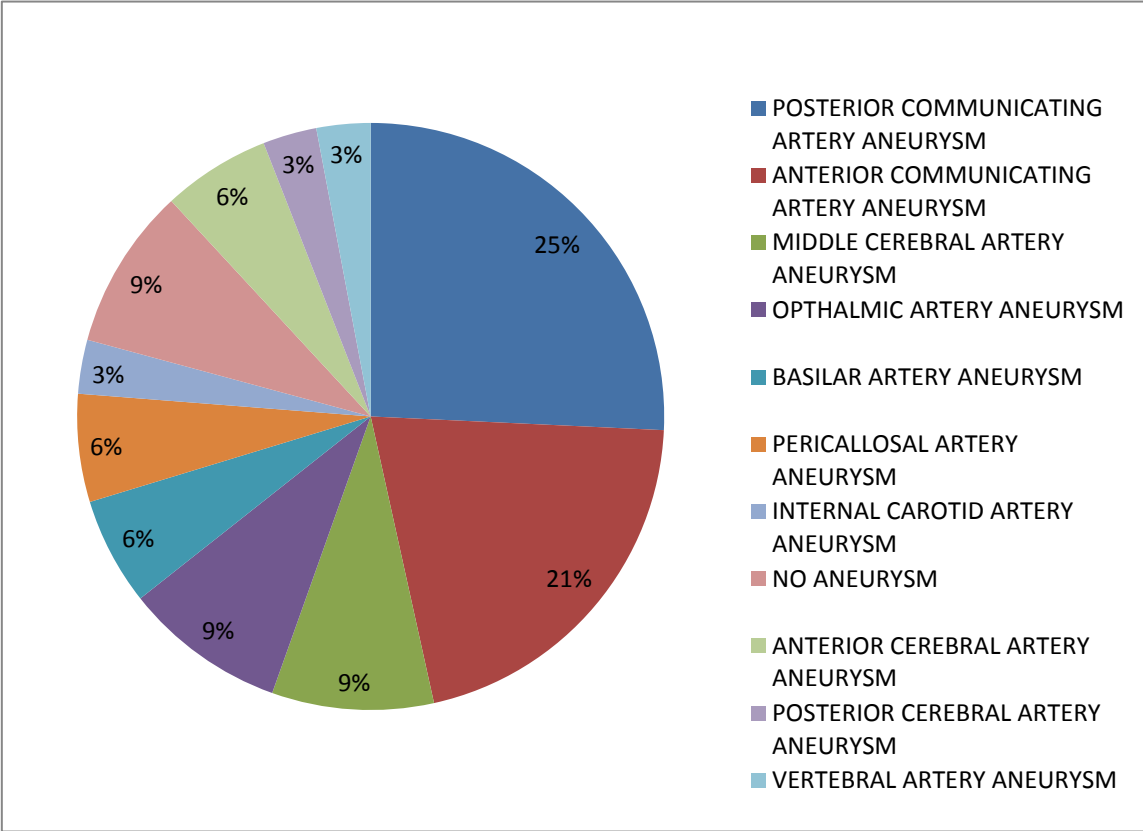


**Figure 4.6: Aneurysm location distribution**

The average thyroid absorbed doses and average KAP values for some of the aneurysm locations are listed in Table 4.6. As can be seen in Table 4.6, the average KAP values for posterior cerebral aneurysms, anterior communicating aneurysms and pericallosal aneurysm coil embolizations were higher compared to the doses received from coiling of aneurysms in other locations. The vertebral artery aneurysm coiling resulted in the highest average thyroid doses followed by the anterior cerebral aneurysm coiling. A Kruskal Wallis test was performed to

determine whether there was a statistically significant relationship between aneurysm location and radiation dose to patients during intracranial aneurysm coiling. This statistical test showed no statistically significant relationship between aneurysm location and thyroid dose ( $p = 0.56$ ) or between aneurysm location and KAP value ( $p = 0.13$ ).

**Table 4.6: The average thyroid absorbed doses and KAP values for different aneurysm locations**

ANEURYSM LOCATION	NUMBER OF CASES	AVERAGE THYROID ABSORBED DOSE (mGy)	AVERAGE KAP (Gy.cm <sup>2</sup> )
Posterior communicating artery aneurysm	9	10.4	44.3
Anterior communicating artery aneurysm	7	13.1	73.1
Middle cerebral artery aneurysm	3	12.4	54.2
Ophthalmic artery aneurysm	3	11.7	45.8
Pericallosal artery aneurysm	2	14.4	71.4
Anterior cerebral artery aneurysm	2	15.3	50.9
Basilar artery aneurysm	2	7.4	59.0
Internal carotid artery aneurysm	1	4.0	68.8
Posterior cerebral artery aneurysm	1	9.7	79.8
Vertebral artery aneurysm	1	18.0	33.3

#### 4.7. Diagnostic reference levels

Diagnostic reference levels were introduced by the ICRP in 1996 for diagnostic radiology and nuclear medicine procedures with the aim of identifying and reducing unjustifiable high radiation doses and promoting dose optimization (ICRP, 2001). For adults, DRLs are usually defined for an average-sized person, typically between 70 kg and 80 kg, and are set at a 75 % level of the dose to those patients (Trapp & Kron, 2008:108).

The radiation dose parameter to be used for a DRL depends on the type of examination. For fluoroscopy guided procedures the ICRP (2017) suggests using the KAP, the number of acquired images or frames, fluoroscopy time and cumulative dose when setting DRLs for interventional procedures. In addition to the afore-mentioned parameters, the IAEA (2010) suggests including the complexity of the study when setting DRLs for fluoroscopically guided procedures, as the procedure complexity affects the radiation dose.

One of the objectives of the current study was to establish the DRLs for intracranial aneurysm coil embolization procedures at the research site. As previously stated, the 75<sup>th</sup> percentile of KAP, fluoroscopy time and number of image frames were used to set DRLs, as suggested by ICRP (2017). The established DRL values from the current study are listed in Table 4.7.

**Table 4.7: DRLs for intracranial aneurysm coil embolizations**

Parameter	Median	75 <sup>th</sup> percentile	Range
<b>KAP (Gy.cm<sup>2</sup>)</b>	52.1	68.8	3.0–125.7
<b>Fluoroscopy time (minutes)</b>	17.8	30.0	4.9–48.3
<b>Number of image frames</b>	504.0	616.0	314.0–1212.0



#### 4.8. Correlation between KAP and the number of image frames

Spearman' correlation coefficient was used to determine whether there was a relationship between KAP and number of image frames. The correlation value was 0.502 ( $p = 0.002$ ) which indicates a positive correlation between KAP and number of image frames. The coefficient of determination  $R^2 = 0.533$ . The scatter graph in Figure 4.7 shows the relationship between KAP and the number of image frames.

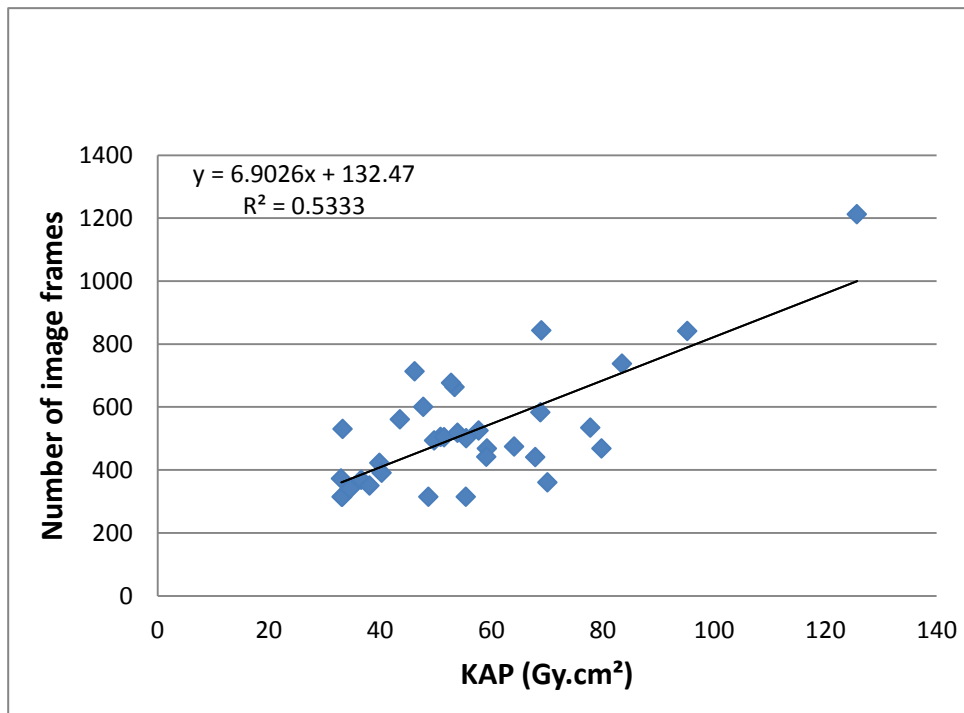


Figure 4.7: Scatter graph showing relationship between KAP and number of image frames

#### 4.9. Correlation between KAP and the maximum entrance skin dose

The maximum entrance skin dose was displayed by the angiography unit for 15 out of the 34 procedures. These entrance skin dose values were used to determine whether there was a correlation between the KAP values and maximum entrance skin dose. The KAP values and maximum entrance skin dose values recorded during the current study are displayed in Table 4.8.

**Table 4.8: KAP and maximum entrance skin dose values**

<b>Study number</b>	<b>KAP (Gy.cm<sup>2</sup>)</b>	<b>Maximum entrance skin dose (mGy)</b>
1	33.1	211
2	95.2	697
3	70.1	458
4	38.1	186
5	55.4	419
6	39.9	194
7	50.9	233
8	79.8	610
9	33.2	263
10	48.7	199
11	33.0	204
12	59.2	454
13	57.7	561
14	53.9	505
15	64.1	214

The correlation value between the KAP and the maximum entrance skin dose was 0.757. This value indicates that there was a positive correlation between the KAP and the maximum entrance skin dose which is stronger than the correlation between the KAP and the number of image frames. The scatter graph in Figure 4.8 shows the relationship between these two variables (KAP and maximum entrance skin dose).

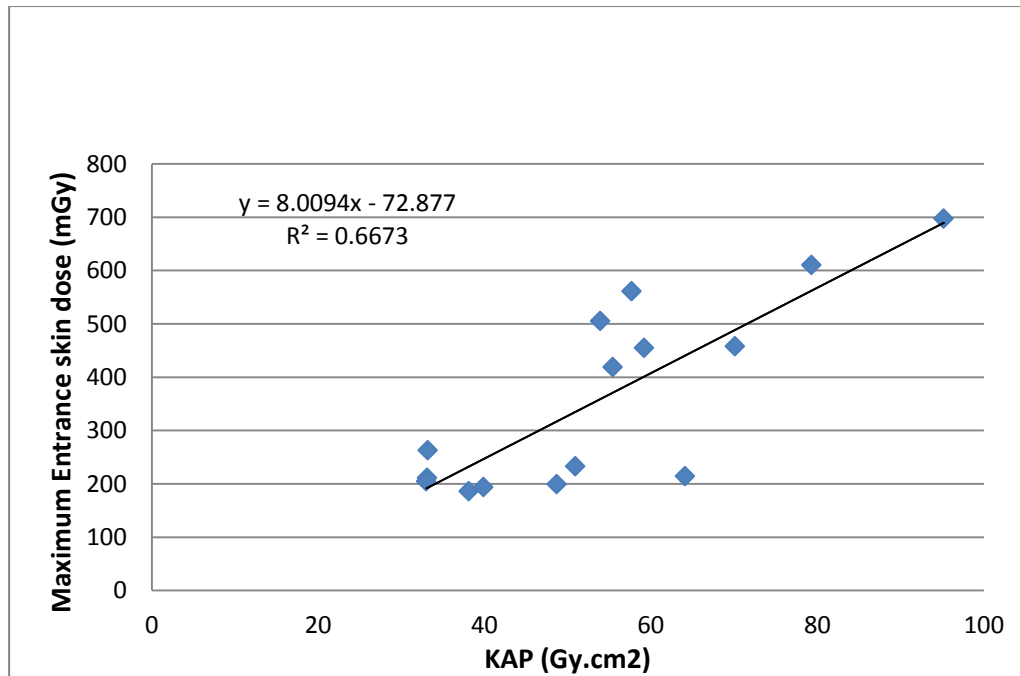


**Figure 4.8: Scatter graph showing positive relationship between KAP and maximum entrance skin dose**

#### 4.10. Conclusion

During this study, the radiation doses to the thyroid glands and skin of patients undergoing intracranial aneurysm coil embolization were measured using TLDs and the KAP meter. The phantom based simulation studies were also performed to determine the difference between the radiation dose measured on the anterior neck and the dose measured directly on the thyroid gland. The average percentage difference between the radiation dose measured on the anterior neck and the dose measured in the thyroid hole of the phantom was found to be 61% and this value was used to calculate the thyroid absorbed doses to participants. In addition to radiation dose measurements, Monte Carlo calculations were also performed after which the calculated doses were compared to the measured doses to determine whether there was correlation between the measured and the calculated doses. The results explained in this chapter will be discussed and compared against similar studies in the following chapter to determine whether the dose values obtained in the current study are comparable to those obtained in other studies.

## **CHAPTER 5: DISCUSSION**

### **5.1. Introduction**

This research study determined the radiation doses to patients' thyroid glands and skin during intracranial aneurysm coil embolizations. DRLs for intracranial coil embolization were also established. Radiation dose measurements during actual coil embolization studies and phantom-based simulation studies were performed using lithium fluoride TLDs and a KAP meter attached to the angiography unit. In this chapter, the results of the current study are discussed and compared to published data related to radiation doses during cerebral embolization procedures.

This study consisted of 34 participants, 30 of whom had intracranial aneurysm coil embolization procedures and 4 of whom had diagnostic cerebral angiography only. The diagnostic cerebral angiography-only procedures were enrolled in the study due to the fact that they were booked as coil embolization procedures. The coil embolization was however not performed on these participants. In three cases, no aneurysms could be identified and in one case the aneurysm was not suitable for coil embolization. On reviewing the data, it was noted that the doses from diagnostic cerebral studies were not significantly different to the doses received during aneurysm coil embolization studies (Table 4.5) and therefore a decision to include diagnostic cerebral cases was reached. However, only the data from coil embolization procedures was used to establish DRLs.

According to Sandborg et al. (2012), intracranial aneurysms are more common in females than in males and occur between the ages of 40 and 60 years. This was also observed in the current study. The research participants included 68% females and 32% males. The age of participants ranged from 18–70 years with the majority of participants (16 out of 34) between the ages of 46 and 55 years. The common anatomical locations for intracranial aneurysms are the anterior communicating artery, origin of posterior communicating artery, middle cerebral artery and basilar artery (Rodriguez-Regent et al., 2014). In this study as well, the most common locations were the origin of the posterior communicating artery (9 out of 30 cases) followed by the anterior communicating artery (7 out of 30 cases).

### **5.2. Sensitivity of TLDs**

TLDs were used for radiation dose measurements during the current study. TLDs are known to have a varying sensitivity to different photon energies. To determine their response or sensitivity

to a certain energy level (tube voltage) and improve their accuracy, TLDs are calibrated for that particular energy level against a measuring instrument of known, reliable standard that has been calibrated (IAEA, 2007). For increased sensitivity to the energy range used during intracranial aneurysm coil embolization, the TLDs that were used in the study were calibrated against an ionization chamber using 70 kV and an air-kerma of 10 mGy (Refer to 3.5.1.1.). These exposures were similar to those employed during intracranial aneurysm coil embolization at the research site. TLD sensitivity is also dependent on the x-ray beam angulation (Bogaert et al., 2009) and this could have affected the accuracy of the results of the current study as multiple different angulations were employed.

### **5.3. Validity and reliability of data**

Measures were taken to ensure validity and reliability of the measurements obtained during the current study. These included ensuring that TLD positioning was the same on all participants during actual coil embolization studies and on the phantom for all simulation studies. Procedures that recorded the shortest fluoroscopy time, the medium fluoroscopy time and the longest fluoroscopy time during the actual coil embolization studies on patients were identified and these scenarios were simulated on the phantom. During the phantom-based simulation studies, each scenario was repeated three times to ensure reliable measurements. Variations in TLD readings and performance of TLD readers also needed to be mitigated for reliable measurements. This could be achieved through routine calibration of the TLDs and TLD readers. To improve accuracy, the TLD reader used for the current study was calibrated for the LiF TLDs before it was used. In addition, TLDs were calibrated and each TLD had its own calibration factor or correction coefficient which was saved on a computer attached to the TLD reader using the TLD number. Saving the calibration factors with the TLD number was done to ensure that a correct calibration factor was used for each TLD every time, thus improving reliability and validity of TLD readings. A standard TLD readout and annealing process (Refer to section 3.7.3) was also followed to ensure reliability of the TLD readings. TLD fading, which can also affect the accuracy of TLD readings, needs to be limited. A study conducted by Good et al. (2013) showed no statistically significant fading on TLDs up to 36 hours after radiation exposure. The TLDs used in the current study were read within 24 hours after radiation exposure to negate possible effects of fading and thus increase the accuracy of the TLD readings.

The KAP was used in the current study to determine the radiation dose to the participants' skin. KAP is associated with an error of between 30% and 40% for skin dose estimation (Miller et al.,

2003; D'Ercole et al., 2007). A 40% error implies that the mean KAP value of 56.1 Gy.cm<sup>2</sup> recorded from the current study could more precisely represent a value of 56.1 Gy.cm<sup>2</sup> ± 22.4, i.e., between 33.7 and 78.4 Gy.cm<sup>2</sup>. The KAP meter that was used for the current study underwent annual calibrations to limit the KAP error to within 25%, as recommended by IAEA (2007). During the 2018 annual KAP meter calibration, the displayed KAP value was found to deviate from the actual value by 6.75% for the plane A KAP meter and 8.79 % for the plane B KAP meter.

In addition to the aforementioned, the research supervisors checked the data on the Excel spreadsheet against the raw data on the data collection sheet to ensure internal validity of the recorded data.

#### 5.4. Thyroid radiation doses

The thyroid absorbed doses obtained during the current study ranged between 3.22 mGy and 20.95 mGy, with a mean thyroid dose of 11.25 mGy. The values recorded in the current study were comparable to thyroid doses reported by Shortt et al. (2007). The thyroid doses reported by Theodorakou and Horrocks (2003) were markedly higher than the results from the current study. The thyroid doses from the current study are compared to the thyroid doses from published studies in Table 5.1.

**Table 5.1: Thyroid doses in cerebral embolizations obtained from the current study and published studies**

Study	Thyroid dose (mGy/mSv)		
	Minimum	Mean	Maximum
<b>Current study</b>	3.22	11.25	20.95
<b>Shortt et al. (2007)</b>	-	8.29	21.00
<b>Theodorakou &amp; Horrocks (2003)</b>	-	24.00	180.00

The radiation effects to the thyroid gland are stochastic in nature, i.e. there is no threshold dose below which they do not occur but the chances of occurrence increase with an increase in the radiation dose. Exposure of the thyroid gland to radiation doses between 50 and 100 mGy has been associated with an increased risk of developing thyroid cancer, especially in children (Sinnott et al., 2010). The thyroid doses found in the current study were below the threshold doses for developing thyroid cancer. This finding suggested that patients exposed to radiation during intracranial aneurysm coil embolization at the research site did not have an increased risk of developing radiation-induced thyroid cancer.

### **5.5. Skin radiation doses**

Radiation doses to patients' skin during the current study were measured using a KAP meter attached to the angiography unit. The KAP values were found to be between 33.0 and 125.7 Gy.cm<sup>2</sup> with the mean value of 56.1 Gy.cm<sup>2</sup>. In addition to recording the KAP values, the maximum entrance skin dose that was displayed by the angiography unit for 15 procedures was also documented. This data was used to determine whether there is correlation between KAP and maximum entrance skin dose and a positive correlation was found. A positive correlation between KAP and maximum skin dose in cerebral angiography and intervention has also been reported in previously published studies (Theodorakou & Horrocks, 2003; D'Ercole et al., 2007; IAEA, 2010; Sandborg et al., 2010). This means that KAP is a useful dose metric that can be used to determine skin dose.

KAP values from the current study and published studies are compared in Table 5.2 and it was seen that the mean KAP value from this study was the lowest among all the listed studies. The minimum KAP for this study was similar to that reported by Papageorgiou et al. (2007) for diagnostic cerebral angiography. The minimum KAP value for diagnostic cerebral angiography in this study was 38.1 Gy.cm<sup>2</sup>, which was slightly higher than the minimum KAP value for coil embolization procedures. The mean KAP values for diagnostic cerebral angiography and coil embolization procedures in this study were 55.1 Gy.cm<sup>2</sup> and 56.3 Gy.cm<sup>2</sup> respectively (Table 4.5). These results supported the argument by Bor et al. (2004) that the complexity of the procedure influenced the radiation dose to the patient more than whether the procedure was diagnostic or therapeutic. This is because for complex procedures longer fluoroscopy times are often employed in attempts to cannulate the arteries of interest and multiple acquisitions are performed to best demonstrate the complex anatomy.

**Table 5.2: KAP values from the current study and published studies**

Study	Procedure type	Sample	KAP (Gy.cm <sup>2</sup> ) Mean (Range)
<b>Current study</b>	Aneurysm embolization	30	56.3 (33.0 – 125.7)
<b>Bor et al. (2005)</b>	Therapeutic	21	215.7 (100.2 – 394.0)
<b>Papageorgiou et al. (2007)</b>	Diagnostic	33	119.0 (33.0 – 261.0)
<b>D’Ercole et al. (2007)</b>	Therapeutic	48	413.0 (81.0 – 1143.0)
<b>Suzuki et al. (2008)</b>	Aneurysm embolization	86	233.0
<b>Sandborg et al. (2010)</b>	Aneurysm embolization	226	(121.0 – 436.0)
<b>Lunelli et al. (2013)</b>	Diagnostic	158	75.4 (16.3 – 251.7)
<b>Ihn et al. (2016)</b>	Aneurysm embolization	371	271.0 (20.0 – 1154.4)
<b>Acton et al. (2018)</b>	Aneurysm embolization	109	108.0 (42.0 – 366.0)

The NCRP (2011) as well as Jaco and Miller (2010) recommend patient follow-up for possible skin injuries for patients exposed to KAP values greater than 500 Gy.cm<sup>2</sup>, while D’Ercole et al. (2007) suggest a threshold dose of 700 Gy.cm<sup>2</sup> for early transient erythema (Table 2.2). The KAP values recorded during the current study were well below these action values and threshold doses. Therefore, it was unlikely that radiation-induced skin injuries could occur to participants following intracranial aneurysm coil embolization at the research site.

### **5.6. Effect of aneurysm location on radiation dose**

One of the objectives of the current study was to determine whether the aneurysm anatomical location affected the radiation dose to patients during intracranial aneurysm coil embolization. Acton et al. (2018) argue that the location of the intracranial aneurysm has an effect on the patient radiation dose, with the coiling of posterior aneurysms resulting in more radiation dose



than coiling of anterior aneurysms. Acton et al. (2018) found the 75<sup>th</sup> percentile KAP value for coiling of anterior aneurysms to be 98 Gy.cm<sup>2</sup>, while it was 151 Gy.cm<sup>2</sup> for posterior circulation aneurysms. D'Ercole et al. (2012), however, found no significant difference in radiation doses resulting from coiling of anterior aneurysms and coiling of posterior aneurysms. In the current study, the mean KAP values recorded for the coiling of posterior cerebral aneurysms and anterior communicating aneurysms were higher than the mean KAP values recorded for the coiling of aneurysms in other anatomical locations. The KAP value resulting from the coiling of posterior cerebral aneurysms was almost double that recorded for posterior communicating artery aneurysms, i.e. 79.8 Gy.cm<sup>2</sup> versus 44 Gy.cm<sup>2</sup>. However, there was no statistically significant relationship between the aneurysm location and the radiation dose ( $p = 0.134$ ). This was thought to be due to the limited sample size, where there was between one and nine sample cases for each aneurysm a location. These results are not statistically reliable therefore future research including a bigger sample size is recommended to evaluate the effect of aneurysm location on radiation dose adequately.

### **5.7. Diagnostic reference levels**

This study determined DRLs for intracranial aneurysm coil embolization using third quartiles of the KAP values, the fluoroscopy time and the number of image frames, as recommended by the IRCP (2017). According to Bogaert et al. (2009), the complexity of the study should also be factored in when setting DRLs for fluoroscopically guided interventional procedures. This, however, was not done for the present study, as the sample size was not large enough to allow for the classification of data according to complexity of the study. DRLs for adults are usually defined for an average-sized person, typically between 70kg and 80kg (Trapp & Kron, 2008:108). The patients' weight was not considered in the current study because Miller et al. (2009) found that the patient's weight did not influence the radiation dose to the patients during cerebral angiography. This may be due to the fact that all human heads are averagely the same size.

Despite the fact that fluoroscopy time has been found to be a poor indicator for the amount of radiation dose received during fluoroscopic procedures (Jaco & Miller, 2010), it is one of the parameters recommended for setting DRLs. The ICRP (2017) argument for inclusion of the fluoroscopy time is that it would be useful in narrowing down the causes of high radiation doses if they occurred. The number of image acquisitions or image frames has been reported to correlate reasonably well with KAP (Theodorakou & Horrocks, 2003; D'Ercole et al., 2012) and

this could explain the relevance of including the number of image frames when setting DRLs for fluoroscopically guided procedures. In the present study, a moderate positive correlation ( $\rho = 0.502$ ) between KAP and number of image frames was also found. This implies that if the KAP is not correlated to the number of image frames, KAP meter recalibration should be performed.

The proposed DRL from this study is 68.6 Gy.cm<sup>2</sup>, 616 image frames and 30 minutes fluoroscopy time. Table 5.3 lists DRLs from the current study and published international peer reviewed studies.

**Table 5.3: Comparison of the DRLs from the current study with DRLs for intracranial aneurysm embolization from published international studies**

Author/ Year of publication	Country	Sample size	Fluoroscopy time (min.) (3 <sup>rd</sup> quartile)	No. of image frames (3 <sup>rd</sup> quartile)	DAP range (Gy.cm <sup>2</sup> )	DRL (Gy.cm <sup>2</sup> ) (3 <sup>rd</sup> quartile)
<b>Current study</b>	South Africa	30	30.0	616.0	33.0–125.7	68.6
<b>Aroua et al., 2007</b>	Switzerland	58	50.0	60.0 - 3348.0 (range)	24.0–1345.0	440.0
<b>Miller et al., 2009</b>	United States of America	148	90.0	1350.0	67.8–825.15	339.4
<b>Sandborg et al., 2010</b>	Sweden	226	7.0–189.0 (range)	Not available	121.0–436.0	157.0
<b>D’Ercole et al., 2012</b>	Italy	72	46.2	664.0	717.0	486.11
<b>Söderman et al., 2013</b>	Sweden	38	16.0	845.0	8.0–635.0	196.0
<b>Erskine et al., 2014</b>	Australia	91	32.0	Not available	Not available	152.9
<b>Chun et al., 2014</b>	Korea	111	61.0	276.0	Not available	272.8
<b>Ihn et al., 2016</b>	Korea	371	64.7	567.3	20.0–1154.4	271.0

As shown in Table 5.3, the KAP value from the current study was lower than those published in the literature. The third quartile of the fluoroscopy time from the current study is double that

reported by Söderman et al. (2013), comparable to that reported by Erskine et al. (2014) and less than half of that reported by Miller et al. (2009), Chun et al. (2014) and Ihn et al. (2016). The number of image frames for the current study was higher than those reported by Chun et al. (2014) and Ihn et al. (2016). A limited number of previous studies on DRLs for cerebral embolizations in South Africa were found. These include one peer reviewed published study (Makosa & Conradie, 2015) and Masters' thesis. The DRLs from these studies are compared against DRLs from the current study in Table 5.4.

**Table 5.4: Comparison of the DRLs from the current study with DRLs for cerebral embolization from South Africa**

Study	Type of procedure	KAP mean (Gy.cm <sup>2</sup> )	75 <sup>th</sup> percentile KAP (Gy.cm <sup>2</sup> )
<b>Current study</b>	Aneurysm embolization	56.3	68.1
<b>Makosa &amp; Conradie, 2015</b>	Cerebral interventions	Not available	200.0
<b>De Vos, 2015</b>	Cerebral interventions	177.8	Not available

There was a wide variation in the third quartile KAP values for cerebral embolization procedures, as can be seen in Tables 5.3 and 5.4. These variations could be as a result of different imaging protocols, different imaging equipment, as well as the experience of the neuro-interventionalists conducting the examinations.

### **5.8. Comparison between measured and calculated doses**

Another objective of the current study was to compare the measured thyroid and skin doses to the calculated doses. The results showed no agreement between the measured thyroid dose and the calculated thyroid dose. The TLD measured thyroid doses ranged between 3.22 and 20.95 mGy while the Monte Carlo calculated doses ranged between 4.50 and 40.47 mGy. There was also no correlation between the calculated thyroid dose and the KAP values despite the fact that the KAP was the dose quantity that was entered in PCXMC for dose calculations. The reason for the poor correlation between the calculated thyroid dose and KAP or measured thyroid dose was thought to be the fact that the thyroid gland was not in the primary beam for

most of the radiation exposures. Different beam angulations were also used with the x-ray beam angled away from the thyroid gland for some radiation exposures. Foerth et al. (2015) found a difference of up to a factor of four between the TLD measurements and Monte Carlo calculated doses for certain organs including the uterus and gonads. The red bone marrow dose from the TLD measurements was 36.6 mSv while the Monte Carlo calculated dose was 70.4 mSv. These authors attributed the difference between the measured and the calculated doses to the difference in construction and geometrical shapes of phantoms. The afore-mentioned studies suggest that the Monte Carlo calculations over-estimate the organ doses. There was however strong positive correlation between measured and calculated skin doses. Peters (2017) also found a positive linear relationship between DAP and Monte Carlo calculated skin dose for barium studies. This indicates that Monte Carlo calculations can be used for determining skin doses while it seems to be inaccurate in estimating other organ doses. Use of TLDs for direct measurement of thyroid doses in human beings is not possible as the thyroid gland is an internal organ. To the researcher's knowledge, a straightforward method of accurately determining thyroid absorbed doses in human beings during intracranial aneurysm coil embolization does not exist. Therefore, the method employed and / or the percentage difference obtained during the phantom based simulation studies performed as part of this research are recommended for use when thyroid absorbed dose data is required.

## **5.9. Conclusion**

Radiation protection, an important aspect of all radiology departments, aims at reducing the radiation dose to patients to the lowest possible values without compromising the image quality. Radiation protection in medicine is underpinned by the principles of justification and optimization of exposure (ICRP, 2007). One of the methods of applying the optimization principle is through the use of DRLs. DRLs are established at national, regional and hospital levels, with hospitals comparing their DRLs to regional or national DRLs (IAEA, 2016).

In the absence of national DRLs, international guidelines can be used for setting and comparing hospital DRLs. In South Africa, there is a paucity of DRLs for fluoroscopically guided procedures, despite a directive from the Radiation Control Directorate of the South African Department of Health for all radiology departments to establish DRLs for all radiological examinations and procedures.

The reviewed literature showed a large variation in DRLs for cerebral embolization, even for the same procedures, e.g. intracranial aneurysm coiling, presumably due to different imaging protocols at different hospitals, different equipment and different operator experience. This wide distribution of DRLs suggests that it is of utmost importance to set DRLs at the hospital level, in addition to the national and regional DRLs. Intracranial aneurysm coil embolization procedures have an increased risk of causing deterministic effects to the patients' skin. These include early transient erythema at doses over 2 Gy and temporary epilation at radiation doses over 3 Gy (ICRP, 2007).

The current study investigated the radiation doses to patients' skin using KAP meters and the thyroid absorbed doses were calculated from the TLD measurements obtained on the anterior neck of patients. Phantom based simulation studies were performed to determine the difference between the radiation dose measured on the anterior neck and the dose on the thyroid gland. The thyroid gland doses were higher than the anterior neck doses as the x-ray beam was attenuated before reaching the anterior neck due to the fact that images were acquired in the postero-anterior and lateral projections. DRLs for intracranial aneurysm coil embolizations at the research site were also established.

The thyroid absorbed doses ranged between 3.22 and 20.95 mGy with a mean of 11.25 mGy. The KAP values ranged between 33 and 125 Gy.cm<sup>2</sup>. The DRL established during this study was 68 Gy.cm<sup>2</sup>, 616 image frames and 30 minutes of fluoroscopy time. Skin and thyroid radiation dose calculations were also performed using the PCXMC program. The measured skin doses and thyroid doses were compared to the PCXMC calculated doses. There was a strong positive correlation between KAP measured and PCXMC calculated skin doses while there was no correlation between thyroid doses calculated from the TLD measurements and the thyroid doses calculated using the PCXMC program.

The radiation doses recorded during the present study are lower than those reported in most published studies for similar procedures. These low doses could be attributed to the dose optimization techniques employed at the research site during cerebral angiography and embolization, as well as the dose reduction technologies incorporated in the angiography unit that were used for these procedures. The procedures were performed by a neuro-interventional fellow under the direct supervision of one of the two experienced neuro-interventionalists with approximately 15 years of experience. The procedures that were considered as complex or difficult were performed by one of the experienced neuro-interventionalists. This might have also

contributed to the low doses reported in this study. The results of this study imply that patients who undergo intracranial aneurysm coil embolization at the research site are not at risk of developing radiation-induced skin injuries.

Radiation doses to the patients' skin and thyroid glands during intracranial aneurysm coil embolization procedures, were measured using KAP meters and TLDs. These doses were compared to the skin and thyroid doses that were calculated using the PCXMC program. The DRLs for intracranial aneurysm coil embolization procedures, at the research site were also established. The results of this research study cannot be generalized to all hospitals that perform intracranial aneurysm coil embolizations in the province of the Western Cape or in South Africa. However, this study can be used as a guide for developing DRLs in other hospitals in the province or the country.

#### **5.10. Limitations and recommendations**

The current study had some limitations. These limitations as well as recommendations for future studies are discussed here. One of the limitations was the fact that the researcher had no access to TLDs when the medical physicist, who was also the research supervisor, was not available. This impacted negatively on the sample size obtained for this research study, as some patients who had agreed to be enrolled in the research study had to be excluded due to the unavailability of TLDs. For future studies involving use of TLDs, it is recommended that the researcher has full access to the TLDs and gains knowledge on the preparation and proper handling of TLDs before the commencement of such a research project.

Another limitation was the small sample size, which negatively affected assessing the effect of an aneurysm location on the radiation dose which was one of the objectives of the study. This limitation occurred because there was a sample of one to nine cases for the aneurysm locations. Future research should include a bigger sample size for each aneurysm location in order to evaluate adequately the effect of aneurysm location on the radiation dose. The sample size was also not large enough to allow for the complexity of the procedure to be considered when setting DRLs as recommended by the IAEA (2009) for fluoroscopy guided procedures.

The TLDs gave irregular readings during the PBSS which could have influenced the consistency of the overall results of the study. Direct skin dose measurements were not performed; the KAP meter was used instead to estimate the skin dose. KAP is associated with an error of 30–40% for skin dose assessments (Miller et al., 2003; D'Ercole et al., 2007). This statement suggests

that KAP values can only be used to approximate skin doses, as accuracy of results cannot be guaranteed. The maximum entrance skin dose was not displayed for all procedures, and this could have affected the results of the correlation between the maximum entrance skin dose and the KAP.

The height and weight of patients, as well as the x-ray field size were not recorded during data collection for the current study and therefore default phantom weight and height, as well as field size were used for the Monte Carlo calculations. This could have affected the accuracy of the calculated doses as according to Tapiovaara and Siiskonen (2008) the accuracy of the aforementioned parameters is necessary for accurate organ dose calculations.

The third quartile values obtained from this study are recommended for use as initial DRLs for intracranial aneurysm coil embolization at the research site. These DRLs should be reviewed and updated regularly, as suggested in the Bonn Call for Action (WHO, 2014). The difference between the radiation dose measured on the anterior neck and the dose measured directly on the thyroid gland obtained in the current study is recommended for use in future studies involving measurement of the radiation dose to the thyroid gland on human participants.

## REFERENCES

- Acton, H., James, K., Kavanagh, R., O'Tuathaigh, C., Moloney, D., Wyse, G., Fanning, N., Maher, M. & O'Connor, O. 2018. Monitoring neurointerventional radiation doses using dose-tracking software: implications for the establishment of local diagnostic reference levels. *European Radiology*, 28(9):3669–3675.
- Acun, H., Kemikler, G. & Karadeniz, A. 2007. Dosimetric analysis of thyroid doses from total cranial irradiation. *Radiation Protection Dosimetry*, 123(4):498–504.
- Allisy-Roberts, P. & Williams, J. 2008. *Farr's physics for medical imaging*. 2<sup>nd</sup> ed. London: Saunders Elsevier.
- Aroua, A., Rickli, H., Stauffer, J., Schnyder, P., Trueb, P., Valley, J., Vock, P. & Verdun, F. 2007. How to set up and apply reference levels in fluoroscopy at a national level. *European Radiology*, 17:1621–1633.
- Balter, S., Fletcher, D., Kuan, H.M., Miller, D., Richter, D., Seissl, H. & Shope, T.B. 2002. Techniques to estimate radiation dose to skin during fluoroscopically guided procedures. *American Association of Physics in Medicine*. <https://www.aapm.org/meetings/02am/pdf/8368-40188.pdf> [15 November 2018].
- Bhatt, B.C. & Kulkarni, M.S. 2014. Thermoluminescent phosphor for radiation dosimetry. In Singh, H. *Defect and Diffusion Forum*. Vol. 347. Zürich, Switzerland: Trans Tech: 179–227.
- Bhuiyan, S.I, Qronfla, M.M, Abulfaraj, A.A, Kinsara, A.A., Taha, T.M., Molla, N.I. & Elmohr, S.M. 2007. Quality assurance and quality control in TLD measurements. *Proceedings of the Second African International Radiation Protection Association Regional Congress*. Egypt. 22 to 26 April.
- Bogaert, E., Bacher, K., Lemmens, K., Carlier, M., Desmet, W., De Wagter, X., Djjan, D., Hanet, C., Heyndrick, X., Legrand, V., Taeymans, Y. & Thierens, H. 2009. A large scale multicentre study of patient skin doses in interventional cardiology: dose area product action levels and dose reference levels. *British Journal of Radiology*, 82:303–312.
- Bor, D., Cekirge, T., Turan, O., Gülay, M., Onal, E. & Cil, B. 2005. Patient and staff doses in interventional neuroradiology. *Radiation Protection Dosimetry*, 117:62–68.



- Bor, D., Sancak, T., Olgar, T., Elcim, Y., Adanali, A., Sanlidilek, U. & Akyar, S. 2004. Comparison of effective doses obtained from dose-area product and air kerma measurements in interventional radiology. *The British Journal of Radiology*, 77:315–322.
- Burns, N. & Grove, S. 2005. *The practice of nursing research conduct, critique and utilization*. 5<sup>th</sup> ed. St Louis: Elsevier Saunders.
- Bushberg, J.T., Seibert, J.A., Leidholdt, E.M. & Boone, J.M. 2012. *The essential physics of medical imaging*. 3<sup>rd</sup> ed.. Philadelphia: Lippincott Williams and Wilkins.
- Chun, C., Kim, B., Lee, C., Ihn, Y. & Shin, Y. 2014. Patient radiation dose in diagnostic and interventional procedures for intracranial aneurysms: experience at a Single Center. *Korean Journal of Radiology*, 15(6):844–849.
- D’Ercole, L., Mantovani, L., Thyron, F., Bocchiola, M., Azzaretti, A., Di Maria, F., Saluzzo, C., Quaretti, P., Rodolico, G., Scagnelli, P. & Andreucci, L. 2007. A study on maximum skin dose in cerebral embolization procedures. *American Journal of Neuroradiology*, 28:503–507.
- D’Ercole, L., Thyron, F., Bocchiola, M., Mantovani, L. & Klersy, C. 2012. Proposed local diagnostic reference levels in angiography and interventional neuroradiology and a preliminary analysis according to the complexity of the procedures. *Physica Medica*, 28:61–70.
- De Vos, H.J. 2015. Radiation dose optimization in interventional radiology and cardiology using diagnostic reference levels. Unpublished Master’s thesis, University of Cape Town, Cape Town. [https://open.uct.ac.za/bitstream/handle/11427/20928/thesis\\_hsf\\_2016\\_de\\_vos\\_hendrik\\_johannes.pdf?sequence=1](https://open.uct.ac.za/bitstream/handle/11427/20928/thesis_hsf_2016_de_vos_hendrik_johannes.pdf?sequence=1) [14 August 2018].
- Engel-Hills, P. & Hering, E.R. 2001. Dose-area product measurements during barium enema radiograph examinations – a Western Cape study. *South African Medical Journal*, 91(8):693–696.
- Erskine, B., Brady, Z. & Marshall, E. 2014. Local diagnostic reference levels for angiographic and fluoroscopic procedures: Australian practice. *Australian College of Physical Scientists and Engineers in Medicine*, 37:75–82.
- Fernández, S., García-Salcedo, R., Mendoza, J.G., Sanchez-Guzmán, D., Rodríguez, R., Gaona, E. & Montalvo, T.R. 2016. Thermoluminescent characteristics of LiF:Mg,Cu,P and CaSO<sub>4</sub>:Dy for low dose measurement. *Applied Radiation and Isotopes*, 50–55.

Foerth, M., Seidenbusch, M.C., Sadeghi-Azandanyani, M., Lechel, U., Treitl, K.M. and Treitl, M. 2015. Typical exposure parameters, organ doses and effective doses for endovascular aortic aneurysm repair: Comparison of Monte Carlo simulations and direct measurements with an anthropomorphic phantom. *European Society of Radiology*, 25:2617-2626.

Furetta, C. 2003. *Handbook of thermoluminescence*. Singapore: World Scientific.

Hall, E.J. 2012. *Radiobiology for the radiologist*. 7<sup>th</sup> ed. Philadelphia: Lippincott Williams & Wilkins.

Ihn, Y.K., Kim, B., Byun, J., Suh, S.H., Won, Y.D., Lee, D.H., Kim, B.M., Kim, Y.S., Jeon, P., Ryu, C., Suh, S., Choi, D.S., Choi, S.S., Choi, J.W., Chang, H.W., Lee, J., Kim, S.H., Lee, Y.J., Shin, S.H., Soo Mee Lim, S.M., Yoon, W., Jeong, H.W. & Han, M.H. 2016. Patient radiation exposure during diagnostic and therapeutic procedures for intracranial aneurysms: a multicenter study. *Neurointervention*, 11:78–85.

International Atomic Energy Agency. 2010. Patient Dose Optimization in Fluoroscopically Guided Interventional Procedures. [14 August 2018].

International Atomic Energy Agency (IAEA). 2007. Dosimetry in diagnostic radiology: an international code of practice. <https://www-pub.iaea.org/MTCD/publications/PDF/TRS457web.pdf> [14 August 2018].

International Atomic Energy Agency (IAEA). 2016. Right dose for accurate diagnosis: track radiation dose to patients and use diagnostic reference levels. <https://www.iaea.org/newscenter/news/right-dose-for-accurate-diagnosis-track-radiation-dose-to-patients-and-use-diagnostic-reference-levels> [28 March 2019]

International Commission on Radiological Protection (ICRP). 2001. Radiation and your patient: diagnostic reference levels in medical imaging – review and additional advice. ICRP Supporting Guidance 2. *Annals of the ICRP*, 31(4):33–52.

International Commission on Radiological Protection (ICRP). 2007. ICRP Publication 103: The 2007 Recommendations of the International Commission on Radiological Protection. *Annals of the ICRP*, 37(2–4):1–332.

International Commission on Radiological Protection (ICRP). 2007. ICRP Publication 105: Radiological Protection in Medicine. *Annals of the ICRP*, 37(5):1–60.

International Commission on Radiological Protection (ICRP). 2012. ICRP Publication 118: ICRP statement on tissue reactions and early and late effects of radiation in normal tissues and organs – threshold doses for tissue reactions in a radiation protection context. *Annals of the ICRP*, 41(1–2):1–322.

International Commission on Radiological Protection (ICRP). 2017. ICRP Publication 135: Diagnostic reference levels in medical imaging. *Annals of the ICRP*, 46(1):1–144.

International Commission on Radiation Units and Measurements (ICRU). 2005. Patient dosimetry for x-rays used in medical imaging. *Journal of the ICRU*, 5(2):1–113.

Jaco, M. & Miller, D. 2010. Measuring and monitoring radiation dose during fluoroscopically guided procedures. *Techniques in Vascular and Interventional Radiology*, 13:188–193.

Kowalczyk, N. 2014. *Radiographic pathology for technologists*. 6<sup>th</sup> ed. Mosby: Elsevier.

Li, Z., Wang, Q., Chen, G. & Quan, Z. 2012. Outcomes of endovascular coiling versus surgical clipping in the treatment of ruptured intracranial aneurysms. *The Journal of International Medical Research*, 40:2145–2151.

Linn-Watson, T. 2014. *Radiographic pathology*. 2<sup>nd</sup> ed. Philadelphia: Lippincott Williams & Wilkins.

Lunelli, N., Houry, H., De Andrade, G.H. & Borrás, C. 2013. Evaluation of occupational and patient dose in cerebral angiography procedures. *Radiol Bras*, 46(6):351–357.

Makosa, F. & Conradie, A. 2015. Diagnostic reference levels for the vascular, screening and adult cardiology units at Universitas Academic Hospital. *Physica Medica*, 31(1):S7.

Maree, K., Creswell, J.W., Ebersöhn, L., Eloff, R., Ferreira, R., Ivankova, N.V., Jansen, J.D., Nieuwenhuis, J., Pietersen, J. & Plano Clark, V.L. 2016. *First steps in research*. 2<sup>nd</sup> ed. Pretoria: Van Schaik.

McParland, B.J. 1998. Entrance skin dose estimates derived from dose-area product measurements in interventional radiological procedures. *British Journal of Radiology*, 71(852):1288–1295.

Meyer, S., Groenewald, W. & Pitcher, R. 2017. Diagnostic reference levels in low- and middle-income countries: early “ALARAM” bells? *Acta Radiologica*, 58(4):442–448.

Miller, D.L., Balter, S., Schueler, B.A., Wagner, L.K., Strauss, K.J. & Vañó, E. 2010. Clinical radiation management for fluoroscopically guided interventional procedures. *Radiology*, 257(2): 321–32.

Miller, D.L., Kwon, D. & Bonavia, G. 2009. Reference levels for patient radiation doses. *Radiology*, 253(3):753–764.

Miller, D., Balter, S., Cole, P., Lu, H., Berenstein, A., Albert, R., Schueler, B., Georgia, J., Noonan, P., Russel, E., Malisch, T., Vogelzang, R., Geisinger, M.m Cardellar, J., St. George, J., Miller, G. & Anderson, J. 2003. Radiation doses in interventional radiology procedures: The Rad IR study part II: kin ose. . *Journal of Vascular Interventional Radiology*, 14(8):977–990.

Muhammad, W., Hussain, A. & Maqbool, M. 2017. Basic concepts in radiation dosimetry. In Maqbool, M. (ed.). *An introduction to medical physics*. Basel, Switzerland: Springer:

Muller, H. 2014. Patient radiation dose ranges for procedures in Universitas Hospital vascular laboratories. Unpublished Master's thesis, Central University of Technology, Bloemfontein.  
<http://ir.cut.ac.za/bitstream/handle/11462/674/Muller%2C%20Henra.pdf?sequence=1&isAllowed=y> [18 October 2016]

Nabasenja, C. 2009. Radiation doses for barium meals and barium enemas in the Western Cape South Africa. Unpublished Master's thesis, Cape Peninsula University of Technology, Cape Town.  
<http://etd.cput.ac.za/bitstream/handle/20.500.11838/1560/fulltext.pdf?sequence=1&isAllowed=y> [18 June 2018].

National Council on Radiation Protection and Measurements. 2011. Radiation dose management for fluoroscopically guided interventional medical procedures. *NRCP Report number 168*. Bethesda, Maryland, United States of America.

Nyathi, T. 2012. Dose optimization in diagnostic radiology. Unpublished PhD thesis, University of the Witwatersrand, Johannesburg.  
<http://mobile.wiredspace.wits.ac.za/bitstream/handle/10539/12706/Dose%20optimization.pdf?sequence=1&isAllowed=y> [18 June 2018].

Papageorgiou, E., Tsapaki, V., Tsalafoutas, I., Maurikou, E., Kottou, S., Orfanos, A., Karidas, G., Fidanis, T., Zafiriadou, E. & Neofotistou, V. 2007. Comparison of patient doses in interventional radiology procedures performed in two large hospitals in Greece. *Radiation Protection Dosimetry*, 124(2):97–102.

Peat, J. & Barton, B. 2005. *Medical statistics: a guide to data analysis and critical appraisal*. Oxford: Blackwell.

Peters, N.B. 2017. Determination of effective dose and entrance skin dose from dose area product values for barium studies in adult patients at a large tertiary hospital in the Western Cape. Unpublished Master's thesis, Cape Peninsula University of Technology, Cape Town. <http://etd.cput.ac.za/bitstream/handle/20.500.11838/2627/191050881-Peters-Nazlea%20Behardien-MSc-Radiography-HWSci-2018.pdf?sequence=1&isAllowed=y> [20 January 2018].

Rampado, O. & Ropolo, R. 2005. Entrance skin dose distribution maps for interventional neuroradiological procedures: a preliminary study. *Radiation Protection Dosimetry*, 117(1):256–259.

Richardson, D. 2009. Exposure to ionizing radiation in adulthood and thyroid cancer incidence. *Epidemiology*, 20:181–187.

Rodriguez-Regent, C., Edjlali-Goujon, M., Trystram, D., Boulouis, G., Ben Hassen, W., Godon-Hardy, S., Nataf, F., MacHet, A., Legrand, L., Ladoux, A., Mellerio, C., Souillard-Scemama, R., Oppenheim, C., Meder, J.F. & Naggara, O. 2014. Non-invasive diagnosis of intracranial aneurysms. *Diagnostic and Interventional Imaging*, 95(12):1163–1174.

Rybicki, F., Nawfel, R., Judy, P., Ledbetter, S., Dyson, R., Halt, P., Shu, K. & Nunez Jr, D. 2002. Skin and thyroid dosimetry in cervical spine screening: two methods for evaluation and a comparison between a helical CT and radiographic trauma series. *American Journal of Radiology*, 179:933–937.

Sandborg, M., Nilsson Althén, J., Pettersson, H. & Rossitti, S. 2012. Patient organ radiation doses during treatment for aneurysmal subarachnoid hemorrhage. *Clinical Neuroradiology*, 22(4):315–325.

- Sandborg, M., Rossitti, S. & Pettersson, H. 2010. Local skin and eye lens equivalent doses in interventional neuroradiology. *European Radiology*, 20(3):725–733.
- Shortt, C.P., Fanning, N.F., Malone, L., Thornton, J., Brennan, P. & Lee, M.J. 2007. Thyroid dose during neurointerventional procedures: does lead shielding reduce the dose? *Cardiovascular and Interventional Radiology*, 30(5):922–927.
- Sinnott, B., Ron, E. & Schneider, B. 2010. Exposing the thyroid to radiation: a review of its current extent, risks and implications. *Endocrine Reviews*, 31(5):756–773.
- Söderman, M., Mauti, M., Boon, S., Omar, A., Marteinsdóttir, M., Andersson, T., Holmin, S. & Hoornaert, B. 2013. Radiation dose in neuroangiography using image noise reduction technology: a population study based on 614 patients. *Neuroradiology*, 55:1365–1372.
- South Africa. Department of Health Directorate: Radiation Control. 2012. Requirements for licence holders with respect to quality control tests for Diagnostic x-ray imaging systems. Pretoria.
- South Africa. Department of Health Directorate: Radiation Control. 2015. Code of practice for users of medical x-ray equipment. Pretoria.
- South African Medical Research Council. 2002. Guidelines on Ethics for Medical Research: Use of Biohazards and Radiation. Cape Town: South African Medical Research Council.
- Suzuki, S., Furui, S., Matsumaru, Y., Nobuyuki, S., Ebara, M., Abe, T. & Itoh, D. 2008. Patient skin dose during neuroembolization by multiple-point measurement using a radiosensitive indicator. *American Journal of Neuroradiology*, 29:1076–1081.
- Tapiovaara, M. & Siiskonen, T. 2008. *PCXMC. A Monte Carlo program for calculating patient doses in medical x-ray examinations*. 2<sup>nd</sup> edition. STUK - A231, Helsinki.
- Theodorakou, C. & Horrocks, J.A. 2003. A study on radiation doses and irradiated areas in cerebral embolization. *British Journal of Radiology*, 76:546–552.
- Trapp, V. & Kron, T. 2008. *An introduction to radiation protection in medicine*. New York: Taylor & Francis.
- Vaz, P. 2014. Radiation protection and dosimetry issues in the medical applications of ionizing radiation. *Radiation Physics and Chemistry*, 104:23–30.

Verdun, F., Aroua, A., Trueb, R., Vock, P. & Valley, J. 2005. Diagnostic and interventional radiology: a strategy to introduce reference dose levels taking into account the national practice. *Radiation Protection Dosimetry*, 114:188–191.

World Medical Association (WMA). 2013. Declaration of Helsinki Ethical Principles for Medical Research Involving Human Subjects. <https://www.wma.net> [8 March, 2019].

World Health Organization (WHO). 2014. Bonn Call for Action. 10 Actions to improve radiation protection in medicine in the next decade.

[www.who.int/ionizing\\_radiation/medical\\_exposure/bonncallforaction2014.pdf](http://www.who.int/ionizing_radiation/medical_exposure/bonncallforaction2014.pdf) [9 December 2017].

Zhao, J., Lin, H., Summers, R., Yang, M., Cousins, B. & Tsui, J. 2018. Current treatment strategies for intracranial aneurysms. *Angiology*, 69(1):17–30.

# APPENDICES

Appendix A: Ionization chamber and electrometer calibration certificates

Appendix B1: Actual coil embolization study data collection sheet

Appendix B2: Phantom based simulation study data collection sheet

Appendix C1: CPUT ethics certificate

Appendix C2: UCT ethics certificate

Appendix C3: Hospital ethics permission certificate

Appendix D: Informed consent form



# NACHWEIS DER KALIBRIERUNG *Certificate of Calibration*



Interne Ref. Nr. / Internal Ref. No. 1702618

PTW-Freiburg, Lörracher Str. 7, 79115 Freiburg, Germany ☎ +49-(0)761- 49055-0 FAX +49-(0)761- 49055-70 E-Mail info@ptw.de

## **Elektrometer / Electrometer : UNIDOS [REF] T10002 [SN] 020016**

Hiermit wird bestätigt, dass das oben genannte Messsystem unter Beachtung eines Qualitätssicherungssystems nach **DIN EN ISO 9001:2008** kalibriert wurde.

Die für die Kalibrierung verwendeten Messeinrichtungen werden regelmäßig kalibriert und sind rückführbar auf die nationalen Normale der Physikalisch Technischen Bundesanstalt (PTB).

Das Gerät entspricht vollständig den Spezifikationen des Datenblatts und der Gebrauchsanweisung.

Das Gerät ist erfolgreich auf seine elektrische Sicherheit gemäß IEC 61010-1 und IEC 60601-1 geprüft worden.

Die für diesen Vorgang angefertigte Dokumentation kann bei Bedarf eingesehen werden.

Die Abweichungen liegen in allen Bereichen unterhalb von 0,5 % (  $k_{elec} = 1.000$  )

Der Selbstablauf während der Kalibrierung war  $\leq \pm 1,0 \cdot 10^{-15}$  A

Die Genauigkeit der Verhältnisse zwischen je zwei Kammeranspannungen waren  $\leq 0,5$  %

*We hereby confirm that the above mentioned measuring system was calibrated according to **DIN EN ISO 9001:2008** under the observation of a certified quality assurance system.*

*The measuring installations used for calibration are regularly calibrated. The calibration of these systems is traceable to standards of the German National Laboratory (PTB).*

*The instrument fully complies with the specifications given in the data sheet and the user manual.*

*The instrument has been successfully checked for electrical safety acc. IEC 61010-1 und IEC 60601-1.*

*The documents established for this procedure are available for inspection on request.*

*The deviations in all ranges are below 0.5 % (  $k_{elec} = 1.000$  )*

*Leakage during calibration was  $\leq \pm 1.0 \cdot 10^{-15}$  A*

*The precision of the relations between bias voltages was  $\leq 0.5$  %*

Freiburg, 21-Jun-2017

PTW-Freiburg  
Physikalisch-Technische  
Werkstätten Dr. Pychlau GmbH

(Unterschrift/Signature)

# CALIBRATION CERTIFICATE

No. 1702618



PTW-Freiburg, Lörracher Str. 7, 79115 Freiburg, Germany ☎ +49-(0)761- 49055-0 FAX +49-(0)761- 49055-70 E-Mail info@ptw.de

## Calibration Object

Radiation Dosimeter  
Elektrometer **UNIDOS [REF] T10002 [SN] 020016**  
Detector **[REF] TW23361 [SN] 000431**  
Detector Type Ionization Chamber

Manufacturer PTW-Freiburg  
Customer FlowBiomed (PTY) LTD Order No. : R171419  
Private Bag X 9 Order Date : 2017-05-31  
ZA-2010 Benmore

## Calibration Results

Measuring Quantity Air Kerma ( $K_{air}$ )  
Detector Calibration Factor  $N_K = 9.099 \cdot 10^5 \text{ Gy / C}$   
Electrometer Calibration Factor  $K_{elec} = 1.000 \pm 0.5 \%$

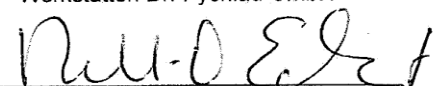
Beam Quality Correction	Beam Quality	Correction Factor $k_Q$	Uncertainty
	N-250	0.995	2.5 %
	N-200	0.984	2.5 %
	N-150	0.989	2.5 %
	N-100	1.000	2.5 %
	N-80	0.998	2.5 %
	N-60	0.963	2.5 %

Reference Conditions  
Beam Quality: N-100  
Temperature: 293.2 K (20°C)  
Air Pressure: 1013.25 hPa  
Relative Humidity: 50%  
Chamber Voltage/Polarity: + 300 V  
Ion Collection Efficiency: 100 %

Calibration Date **2017-06-20**  
Recalibration Interval 2 years (recommended)

Freiburg, 2017-06-21

PTW-Freiburg  
Physikalisch-Technische  
Werkstätten Dr. Pychlau GmbH

  
(Signature)

**B1: ACTUAL COIL EMBOLIZATION STUDY DATA COLLECTION SHEET**

STUDY NO.	GENDER	AGE	ANEURYSM LOCATION	kV	DAP (cGy.cm <sup>2</sup> )	FLUORO TIME (min)	MAXIMUM ENTRANCE SKIN DOSE	NO. OF IMAGE FRAMES	WORKING VIEW	TLD NO.	TLD reading (mGy)	3D ROTATION (Y/N)

**B2: PHANTOM BASED SIMULATION STUDY DATA COLLETION SHEET**

<b>STUDY NO.</b>	<b>WORKING VIEW</b>	<b>FLUORO TIME (Min)</b>	<b>DAP (cGy.cm<sup>2</sup>)</b>	<b>THYROID TLD no.</b>	<b>THYROID TLD READING (mGy)</b>	<b>ANTERIOR NECK TLD no.</b>	<b>ANTERIOR NECK TLD READING (mGy)</b>

**HEALTH AND WELLNESS SCIENCES RESEARCH ETHICS COMMITTEE (HW-REC)**  
Registration Number NHREC: REC- 230408-014

P.O. Box 1906 • Bellville 7535 South Africa  
Symphony Road Bellville 7535  
Tel: +27 21 959 6917  
Email: sethn@cput.ac.za

7 May 2019  
**REC Approval Reference No:**  
**CPUT/HW-REC 2017/H6 (renewal)**

---

Faculty of Health and Wellness Sciences – Medical Imaging and Therapeutic Sciences

Dear Ms Peter

**Re: APPLICATION TO THE HW-REC FOR ETHICS CLEARANCE**

Approval was granted by the Health and Wellness Sciences-REC on 30 March 2017 to Ms Yanda Peter – 201106124 for ethical clearance. This approval is for research activities related to student research in the Department of Medical Imaging and Therapeutic Science at this Institution.

**TITLE: Measurement of the average radiation dose to patients during intracranial aneurysm coiling**

**Supervisor: Mr A Speelman, Mr V Jonas and Ms V Daries**

**Comment:**

**Data collection** permission is required and has been obtained.

Approval will not extend beyond 8 May 2020. An extension should be applied for 6 weeks before this expiry date should data collection and use/analysis of data, information and/or samples for this study continue beyond this date.

The investigator(s) should understand the ethical conditions under which they are authorized to carry out this study and they should be compliant to these conditions. It is required that the investigator(s) complete an annual progress report that should be submitted to the HWS-REC in December of that particular year, for the HWS-REC to be kept informed of the progress and of any problems you may have encountered.

Kind Regards



*Dr. Navindhra Naidoo*  
**Chairperson – Research Ethics Committee**  
Faculty of Health and Wellness Sciences



UNIVERSITY OF CAPE TOWN  
Faculty of Health Sciences  
Human Research Ethics Committee



Room E53-46 Old Main Building  
Groote Schuur Hospital  
Observatory 7925  
Telephone (021) 406 0492  
Email: [surveys@hrifhs.uct.ac.za](mailto:surveys@hrifhs.uct.ac.za)  
Website: [www.health.uct.ac.za/hrs/research/humanethics/forms](http://www.health.uct.ac.za/hrs/research/humanethics/forms)

06 July 2017

**HREC REF: 471/2017**

**Mr A Speelman**  
Division of Radiography  
Block A, Old Education Building  
Cape Peninsula University of Technology  
Bellville

Dear Mr Speelman

**PROJECT TITLE: MEASUREMENT OF AVERAGE RADIATION DOSE TO PATIENTS DURING INTRACRANIAL ANEURYSM COILING- (Master's candidate- Y Peter)**

Thank you for submitting your study to the Faculty of Health Sciences Human Research Ethics Committee (HREC) for review.

It is a pleasure to inform you that the HREC has **formally approved** the above-mentioned study.

**Approval is granted for one year until the 30 July 2018.**

Please include the UCT FHS HREC contact details to the informed consent document.

Please submit a progress form, using the standardised Annual Report Form if the study continues beyond the approval period. Please submit a Standard Closure form if the study is completed within the approval period.

(Forms can be found on our website: [www.health.uct.ac.za/fhs/research/humanethics/forms](http://www.health.uct.ac.za/fhs/research/humanethics/forms))

**We acknowledge that the student, Y Peter will also be involved in this study.**

**Please quote the HREC REF in all your correspondence.**

Please note that the ongoing ethical conduct of the study remains the responsibility of the principal investigator.

Please note that for all studies approved by the HREC, the principal investigator **must** obtain appropriate institutional approval before the research may occur.

Yours sincerely

  
PP **PROFESSOR M BLOCKMAN**  
**CHAIRPERSON, FHS HUMAN RESEARCH ETHICS COMMITTEE**

HREC 471/2017



Western Cape  
Government

Health

Mr A. Speelman  
Division of Radiography  
CAPE PENINSULA UNIVERSITY OF TECHNOLOGY

E-mail: [peterv@cput.ac.za](mailto:peterv@cput.ac.za)

Dear Mr. Speelman

**RESEARCH PROJECT EXTENSION: Measurement of Average Radiation Dose To Patients During Intracranial Aneurysm Coiling (Masters Candidate Ms. Yanda Peters)**

Your recent communication to the hospital refers.

The extension of your research is approved in accordance with UCT Ethics clearance, until 30 July 2019.

As previously mentioned:

- a) Your research may not interfere with normal patient care.
- b) Hospital staff may not be asked to assist with the research.
- c) No hospital consumables and stationary may be used.
- d) **No patient folders may be removed from the premises or be inaccessible.**
- e) Please provide the research assistant/field worker with a copy of this letter as verification of approval.
- f) Confidentiality must be maintained at all times.
- g) Once the research is complete, please submit a copy of the publication or report.

I would like to wish you every success with the project.

Yours sincerely

## **Informed Consent form for participation in a Research Study**

**TITLE OF THE RESEARCH:** MEASUREMENT OF THE AVERAGE RADIATION TO PATIENTS DURING INTRACRANIAL ANEURYSM COILING

**NAME OF RESEARCHER:** YANDA PETER

**NAME OF INSTITUTION:** CAPE PENINSULA UNIVERSITY OF TECHNOLOGY

**This Informed Consent Form has two parts:**

- Information Sheet (to share information about the research with you)
- Certificate of Consent (for signatures if you agree to take part)

**You will be given a copy of the full Informed Consent Form**



## **PART I: Information Sheet**

### **Introduction**

I am Yanda Peter, a Master of Science in Radiography student at the Cape Peninsula University of Technology. As part of my studies, I am doing a research project about radiation dose during intracranial aneurysm coiling, and I would like to invite you to take part in this research.

### **Purpose of the research**

An intracranial aneurysm is the bulging or ballooning of the vessel wall that causes bleeding inside the brain. This bulging of the vessel wall is often caused by the weakening of the blood vessels due to a number of conditions like high blood pressure. Aneurysms can be treated successfully during a procedure called endovascular coiling of the aneurysm. This procedure uses x-rays to help the doctors ensure that the wires are in the correct place and that the coils sit in the aneurysm perfectly. My reason for doing this study is to measure the amount of radiation received by the patients during aneurysm coiling.

### **Type of Research Intervention**

This research will not affect the way in which the normal coiling procedure is done. A radiation measuring device will be placed in the midline of your neck and taped down using sticky tape before the procedure. Immediately after the procedure, the measuring device will be removed from your neck. The measurements on the measuring device will be read using a special dose reading machine to ascertain the amount of radiation dose received. The measuring device will not cause you any discomfort nor does it cause any pain and there are no known side effects associated with it.

### **Voluntary Participation**

I request your participation in this research study. Your participation will be entirely voluntary, that means you can choose whether to participate or not. You have a right to refuse to participate in this study and your refusal will not be used against you. If you

choose to participate, you have a right to withdraw from participating any time, should you wish to do so without any penalties or interruption or deviation of the aneurysm coiling procedure.

### **Risks and Benefits**

There are no risks associated with this research study, there may only be slight discomfort from the measuring device that will be placed on the neck. If you participate in this study, there will be no benefits to you directly but your participation is likely to help us understand the amount of radiation dose the patients receive during endovascular coiling and if necessary find ways of reducing the dose.

### **Confidentiality**

We will make sure that only the research team has access to the information gained from this research. Any information about you will have a number on instead of your name and only the research team will know your number. Your name or the type of disease you have will not be used for this research project. Your name will also not be used or published during the write up of the results.

### **Results of this study:**

You may receive the overall outcome of this study. If you wish, the results will be forwarded to you by mail.

### **Who to Contact**

If you have any questions about this research you may contact the following people:

1. Yanda Peter

Radiography department

Cape Peninsula University of Technology

Tel: 021 959 6538

Email: [petery@cput.ac.za](mailto:petery@cput.ac.za)

2. Mr A. Speelman (Research supervisor)  
Radiography department  
Cape Peninsula University of Technology  
Tel: 021 959 6231  
Email: [speelmana@cput.ac.za](mailto:speelmana@cput.ac.za)

**The research proposal for this study has been reviewed and approved by the Faculty of Health and Wellness Research Ethics Committee at the Cape Peninsula University of Technology, which is a committee whose task it is to make sure that research participants are protected from harm.**

**PART II: Certificate of Consent**

I have read the above information, or it has been read to me. I have had the opportunity to ask questions about it and all my questions have been answered to my satisfaction. I consent voluntarily to participate in this research.

**Print Name of Participant** \_\_\_\_\_

**Signature of Participant** \_\_\_\_\_

**Date** \_\_\_\_\_

**OR**

**Thumb print of participant**

**I would like to receive the overall results of this study:**

<b>YES</b>		<b>NO</b>	
------------	--	-----------	--

I have witnessed the accurate reading of the consent form to the potential participant and I confirm that the individual has given consent freely.

**Print name of witness** \_\_\_\_\_

**Signature of witness** \_\_\_\_\_

**Date** \_\_\_\_\_

**Statement by the researcher/person taking consent**

I have, to the best of my ability, made sure that the participant understands what the research is about, and what to expect. I confirm that the participant was given an opportunity to ask questions about the study, and all the questions asked by the participant have been answered correctly. I confirm that the consent has been given freely and voluntarily.

**A copy of this informed consent form has been provided to the participant.**

**Print Name of Researcher/person taking the consent** \_\_\_\_\_

**Signature** \_\_\_\_\_

**Date** \_\_\_\_\_